

Electronic Supplementary Information

Targeted Drug Delivery in Covalent Organic Nanosheets (CONs) *via* Sequential Postsynthetic Modification

Shouvik Mitra,^a Himadri Sekhar Sasmal,^{a,b} Tanay Kundu,^{a,b} Sharath Kandambeth,^{a,b} Kavya Illath,^{a,b} David Díaz Díaz,^c and Rahul Banerjee^{*a,b}

^a Physical/Materials Chemistry Division, CSIR-National Chemical Laboratory, Pune, India.

^b Academy of Scientific and Innovative Research (AcSIR), New Delhi, India.

^c Institut für Organische Chemie, Universität Regensburg, Universitätsstr.31, 93040 Regensburg, (Germany); and IQAC-CSIC, Jordi Girona 18-26, Barcelona 08034, (Spain).

Section		Page No
S-1	General information	S2
S-2	Synthetic procedures	S2
S-3	Crystallographic details of ligand and monomer	S6
S-4	Structural modeling and Powder X-Ray Diffraction analysis	S8
S-5	Fractional atomic coordinates of unit cells	S10
S-6	Characterization details of the two COFs	S13
S-7	Morphological analysis of the COFs	S15
S-8	Stability study of TpASH	S16
S-9	COF to functionalized CONs <i>via</i> postsynthetic modification steps	S17
S-10	Detailed biological studies	S26
S-11	References	S32

Section S-1: General information

General remarks: 4-Aminosalicylic acid, 4-Aminobenzohydrazide/ 4-Aminophenylhydrazide (APH) was obtained from Sigma Aldrich; *p*-toluenesulphonic acid (PTSA) was purchased from TCI chemicals. All other reagents were of analytical grade and used without further purification. Powder X-ray diffraction (PXRD) patterns were recorded on Phillips PANalytical diffractometer for Cu K α radiation ($\alpha = 1.5406 \text{ \AA}$), with a scan speed of 1° min^{-1} and a step size of 0.02° in 2θ and Rigaku MicroMax 007HF diffractometer respectively. Fourier transform infrared (FT-IR) spectra were recorded on a Bruker Optics ALPHA-E spectrometer with a universal Zn-Se ATR (attenuated total reflection) accessory in the $600\text{--}4000 \text{ cm}^{-1}$. Thermogravimetric analyses (TGA) were carried out on a TG50 analyzer (Mettler-Toledo) under N $_2$ atmosphere with a heating rate of $10 \text{ }^\circ\text{C min}^{-1}$. BET surface of the samples were measured using Quantochrome Autosorb instrument. Prior to surface area analysis the samples were activated at $130 \text{ }^\circ\text{C}$ for 8h. Water uptake capacities of the activated samples were measured after activation of the samples in *Quantachrome Quadrasorb* automatic volumetric instrument (up to 1 bar) at 298 K. SEM images were obtained with a Zeiss DSM 950 scanning electron microscope and FEI, QUANTA 200 3D Scanning Electron Microscope with tungsten filament as electron source operated at 10 kV. The samples were sputtered with Au (nano-sized film) prior to imaging by SCD 040 Balzers Union. TEM images were recorded using FEI Tecnai G2 F20 X-TWIN TEM at an accelerating voltage of 200 kV. For TEM, the samples were sonicated for 45 min in methanol, followed by drop casting the sample on carbon coated copper TEM grids (TED PELLA, INC. 200 mesh). AFM images were recorded using Bruker multimode 8 scanner with Nanoscop V controller. For SEM and AFM the samples were prepared in a similar way. Solid state NMR (SSNMR) of the samples were recorded in Bruker 300 MHz NMR spectrometer. Fluorescence and bright field microscopic images were recorded in BD pathway 855 microscope and optical microscope respectively.

Section S-2: Synthetic procedures

Synthesis of 4-Aminosalicylhydrazide (ASH): ASH was synthesized following a reported procedure. This involved a two step reaction, of which the first step is the conversion of 4-Aminosalicylic acid to subsequent ester; while the second step involves the conversion of ester to 4-Aminosalicylhydrazide.¹
Synthesis of ester: 5g of 4-Aminosalicylic acid was dissolved in about 50 mL of dried ethanol. To it 3 mL of conc. H $_2$ SO $_4$ was added dropwise under cooling condition, the resultant mixture was refluxed for 3h under nitrogen atmosphere. After completion of refluxation, the resultant mixture was allowed to cool down to room temperature. Nearly 30 mL of ethanol was evaporated, and it was neutralized using saturated Na $_2$ CO $_3$ solution. This resulted in a whitish precipitate which was extracted with ethyl acetate

followed by drying them in presence of anhydrous Na_2SO_4 . The resultant solution containing the ester was collected by evaporation of ethyl acetate under vacuum. (Yield: 2.6g, ~50%)

Synthesis of diamine: 2.5 g of Ethyl-4-aminosalicylate was added to about 10 mL of 80% hydrazine monohydrate. The resultant mixture was refluxed for overnight under nitrogen atmosphere. After evaporation of excess hydrazine monohydrate, the product was added to ice cold distilled water, followed by extraction in ethyl acetate. After evaporation of ethyl acetate under vacuum crude ASH was collected and decolorized in hot charcoal-ethanol mixture to yield purified ASH. (Yield: 1g, ~40%)

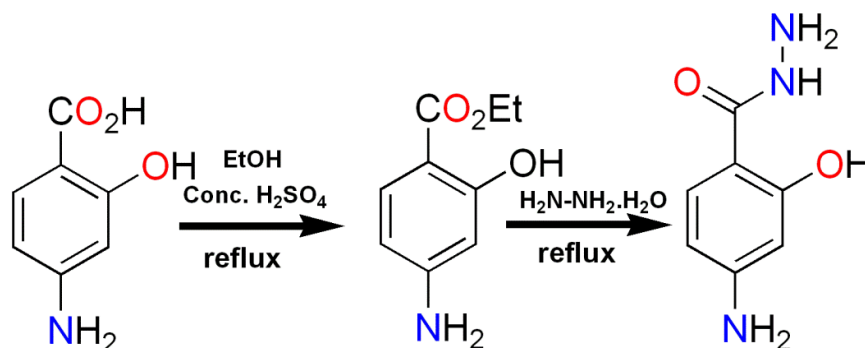


Figure S1. Synthetic scheme of ASH. First step involved formation of ester, while the second step involved conversion of ethyl-4-aminosalicylate to 4-aminosalicylhydrazide.

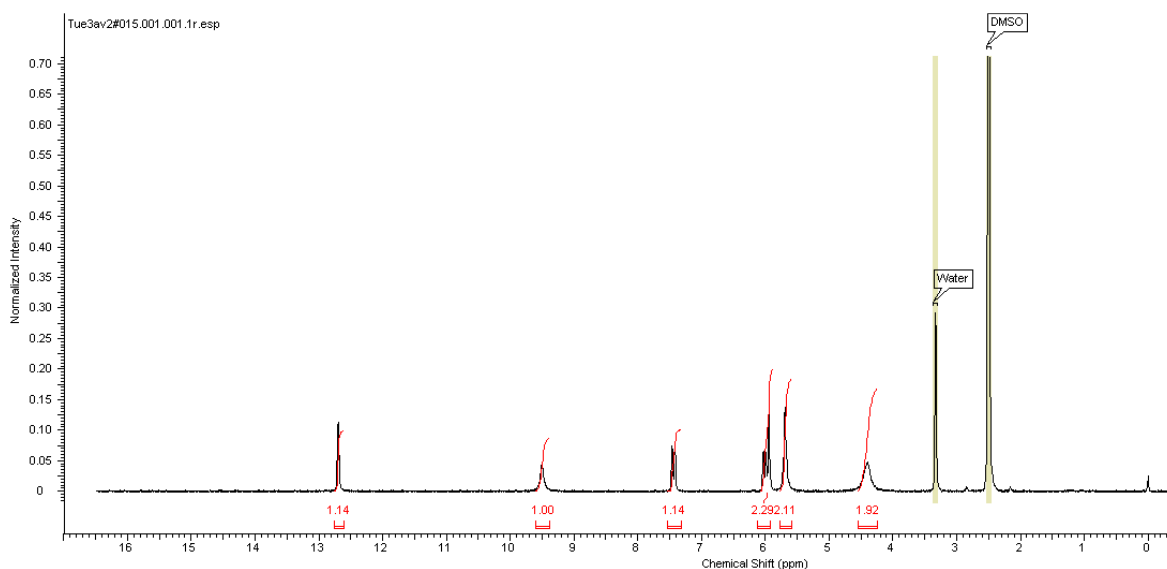


Figure S2. ^1H NMR spectra of ASH in DMSO-d_6 .

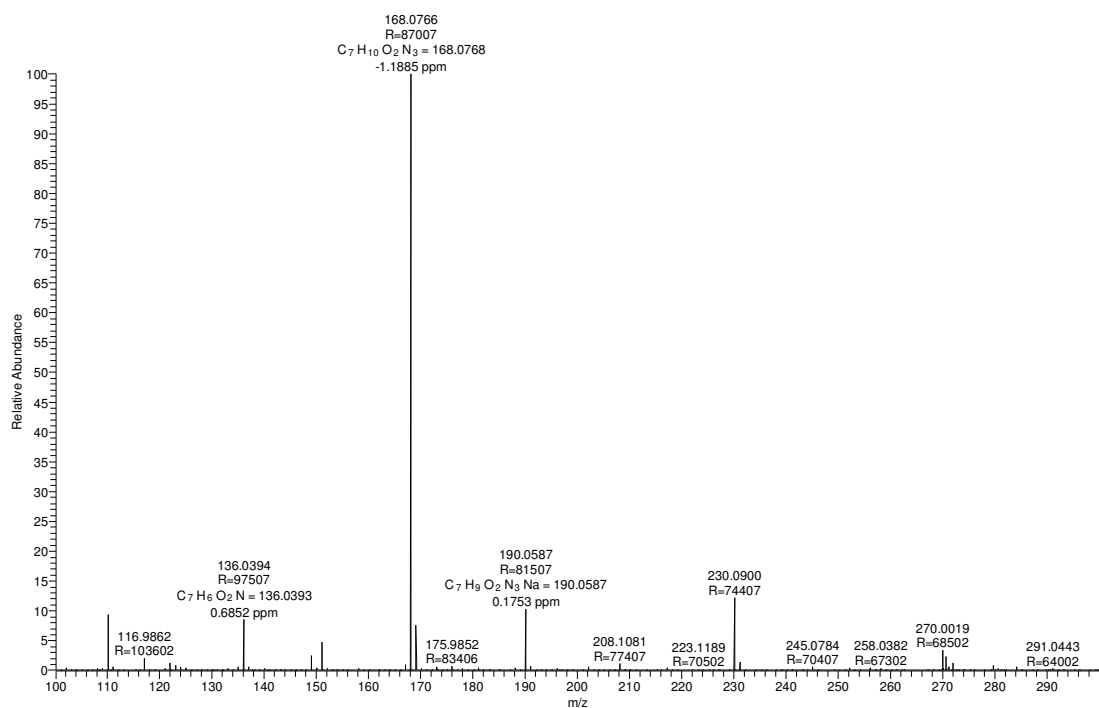


Figure S3. HRMS analysis of ASH which shows the base peak at m/z (M+1).

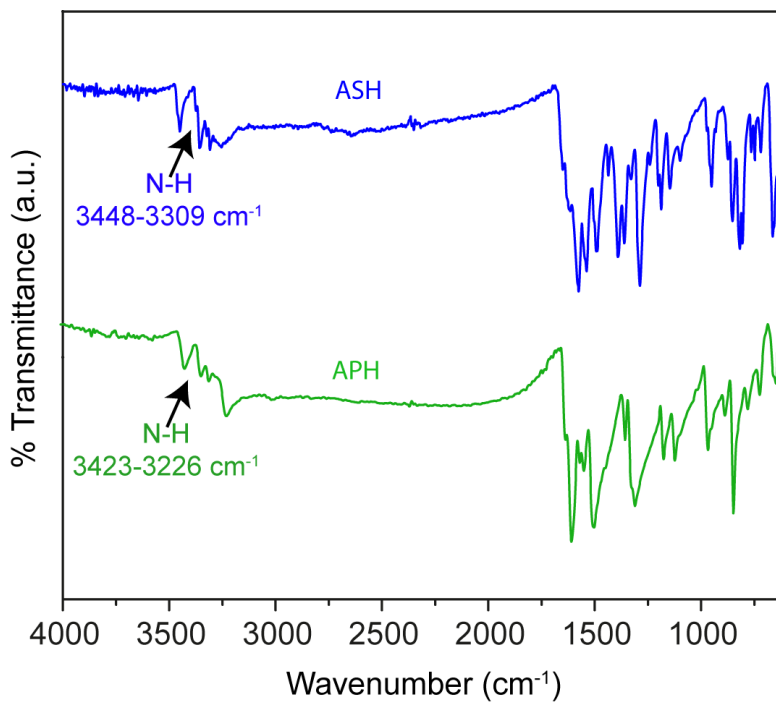


Figure S4. Comparison of FTIR spectra of APH and ASH. Both shows characteristic N-H stretching frequency.

Synthesis of 1,3,5-triformylphloroglucinol (Tp): 1,3,5-Triformylphloroglucinol has been synthesized using our previously reported methods.^{2,3} Briefly, to a mixture of 7.4 g hexamethylenetetramine and 3 g of dried phloroglucinol, trifluoroacetic acid (45 mL) was added. The addition was carried out cautiously under cold condition. The temperature of the mixture was then slowly increased to room temperature. The solution was then allowed to reflux at 100 °C for 2.5 h under nitrogen atmosphere. After that time period 3 M HCl was added to it slowly and was further refluxed for another 1h. Finally, the mixture was allowed to cool to room temperature and filtered through celite bed. Obtained filtrate was extracted with dichloromethane (4 times) and dried over anhydrous Na₂SO₄. The obtained extract was concentrated to yield dull yellow colored solid. Obtained crude product was purified by using hot ethanol to yield the desired product.

Synthesis of COFs: Two COFs (TpAPH and TpASH) were synthesized *via* salt-mediated Schiff base condensation between 0.3 mmol 1,3,5-triformylphloroglucinol (Tp) (63 mg) and 0.45 mmol of diamines (APH: 68 mg, ASH: 75.15 mg) in presense of *p*-toluenesulphonic acid (PTSA) (500 mg). Briefly, the diamines and PTSA were mixed in a pestle mortar for about 10 min to obtain a sticky salt. To it, Tp and de-ionized water were added and mixed. The mixture was then transferred to a glass vial and kept in 90 °C for 12h. After 12h, the vial was taken out from the oven and the resultant product was washed extensively with hot water (to remove PTSA), DMAc and acetone respectively. The product was dried at 90 °C for overnight to obtain brown colored COFs in ~80 % isolated yield. FTIR (ATR, cm⁻¹): TpASH: 1569 (s), 1453 (m), 1352 (w), 1250 (s), 1161 (m), 985 (w), 820 (w), 674 (w). FTIR (ATR, cm⁻¹): TpAPH: 1569 (s), 1453 (m), 1352 (w), 1257 (s), 1181 (m), 988 (w), 846 (w), 814 (w), 748 (w).

Synthesis of TpASH monomer (SaASH) [(4E,10E)-N'-(2-hydroxybenzylidene)-4-(2-hydroxybenzylideneamino)-2-hydroxybenzohydrazide]: 4-Aminosalicylhydrazide (50.1 mg, 0.3 mmol) was dissolved in hot ethanol (20 mL). To it 0.6 mmol 2-hydroxybenzaldehyde was added, and the resultant mixture was refluxed for 6 h. After completion of the reaction yellow colored product was isolated and dried under reduced pressure. Finally the monomer (SaASH) was crystallized by dissolving in hot DMF.

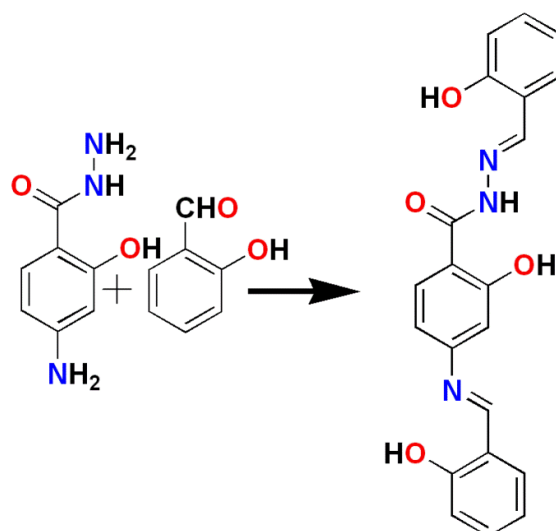


Figure S5. Synthesis scheme of TpASH monomer (SaASH).

Section S-3: Crystallographic details of ligand and monomer

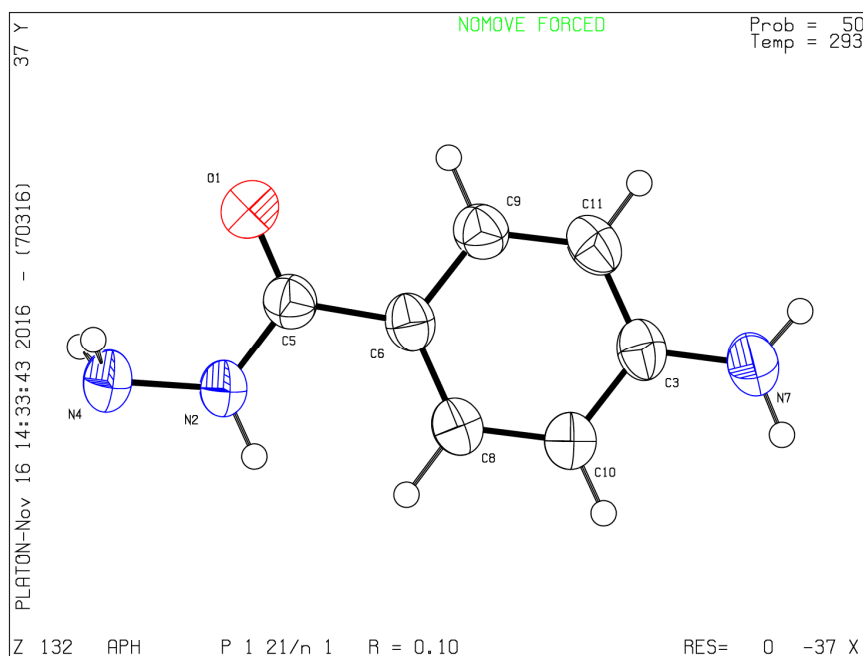


Figure S6. ORTEP diagram of APH at 50% ellipsoid probability level crystallized in $P2_1/n$ space group. Moiety formula $C_7H_9N_3O$, $a = 5.4473(11)$ Å, $b = 13.907(3)$ Å, $c = 10.057(2)$ Å; $\alpha = 90^\circ$, $\beta = 102.69^\circ$, $\gamma = 90^\circ$; cell volume 743.264 [Ref no. CCDC: 1525106]. This crystal is the polymorph of the reported one by Capobianco et al.⁴

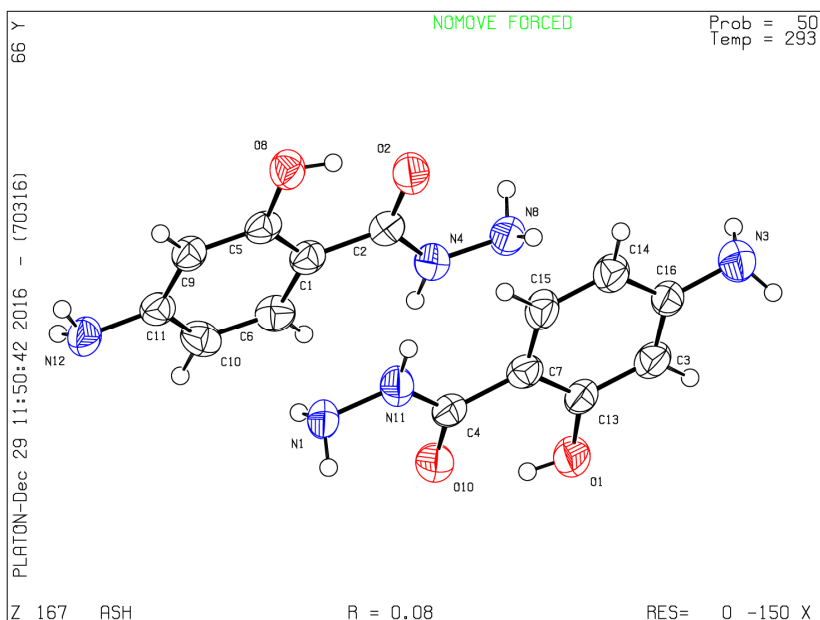


Figure S7. ORTEP diagram of ASH at 50% ellipsoid probability level crystallized in $P2_12_12_1$ space group. Moiety formula $C_7H_9N_3O_2$, $a = 5.7856(8)$ Å, $b = 13.4044(10)$ Å, $c = 19.945(3)$ Å; $\alpha = \beta = \gamma = 90^\circ$; cell volume 1546.78 [Ref. No. **CCDC 1525281**]. This crystal adopt similar geometry to that one reported by Kargar et al.⁵

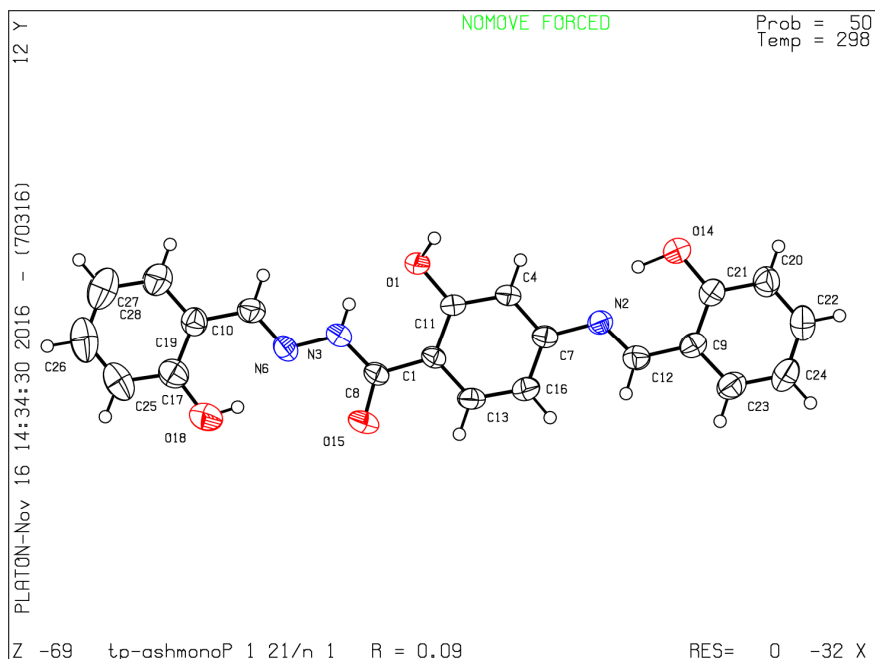


Figure S8. ORTEP diagram of TpASH monomer at 50% ellipsoid probability level. Moiety formula $C_{21}H_{17}N_3O_4$, space group $P2_1/n$, $a = 6.6135(9)$ Å, $b = 36.548(3)$ Å, $c = 7.6248(13)$ Å; $\alpha = 90^\circ$, $\beta = 109.106^\circ$, $\gamma = 90^\circ$; cell volume 1741.47 [Ref. No. **CCDC: 1525107**].

Section S-4: Structural modeling and Powder X-Ray Diffraction analysis

Although these COFs were moderately crystalline materials, still we have tried the 2-D modelling by using Density Functional Tight-Binding method in order to correlate the experimental PXRD pattern with the simulated one. Two possible modelling (AA stacking and AB stacking modes) were considered for the two COFs. Conventional modelling of COFs in AA stacking mode was carried out using hexagonal ($P1$) space group, where PXRD pattern matched well with the simulated one. In contrast, AB staggered modelling was built up using hexagonal ($P6_3$) space group and compared with the simulated PXRD pattern. Refinements of PXRD pattern were done using Pauli refinement of Material studio.⁶

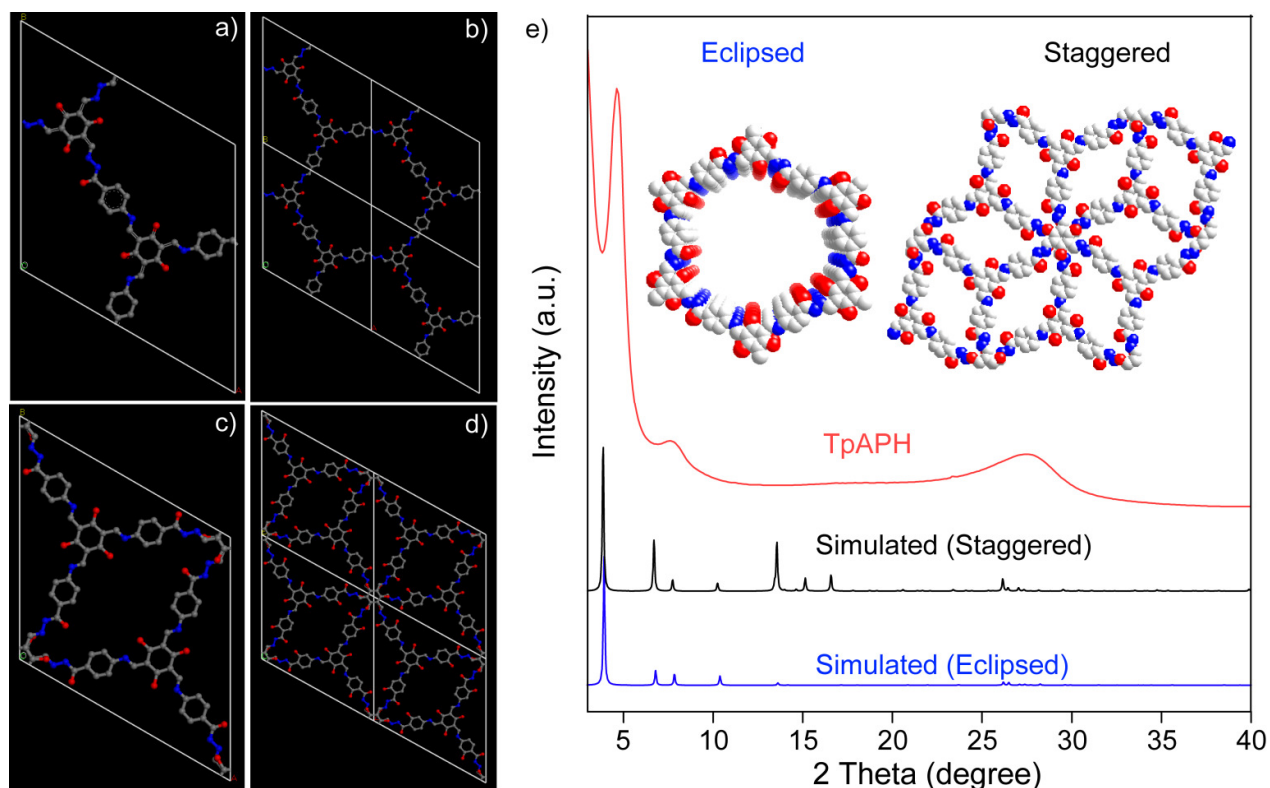


Figure S9. (a) Unit cell and (b) eclipsed crystal lattice packing of TpAPH; (c) unit cell and (d) staggered crystal lattice packing of TpAPH; (e) Comparison of PXRD patterns between TpAPH experimental, staggered (simulated) and eclipsed (simulated). Inset indicate the space-fill modeling of TpAPH COFs in eclipsed and staggered mode. Note: The crystallinity of these COFs reported in this paper are moderate, hence the model structures are approximate and hypothetical.

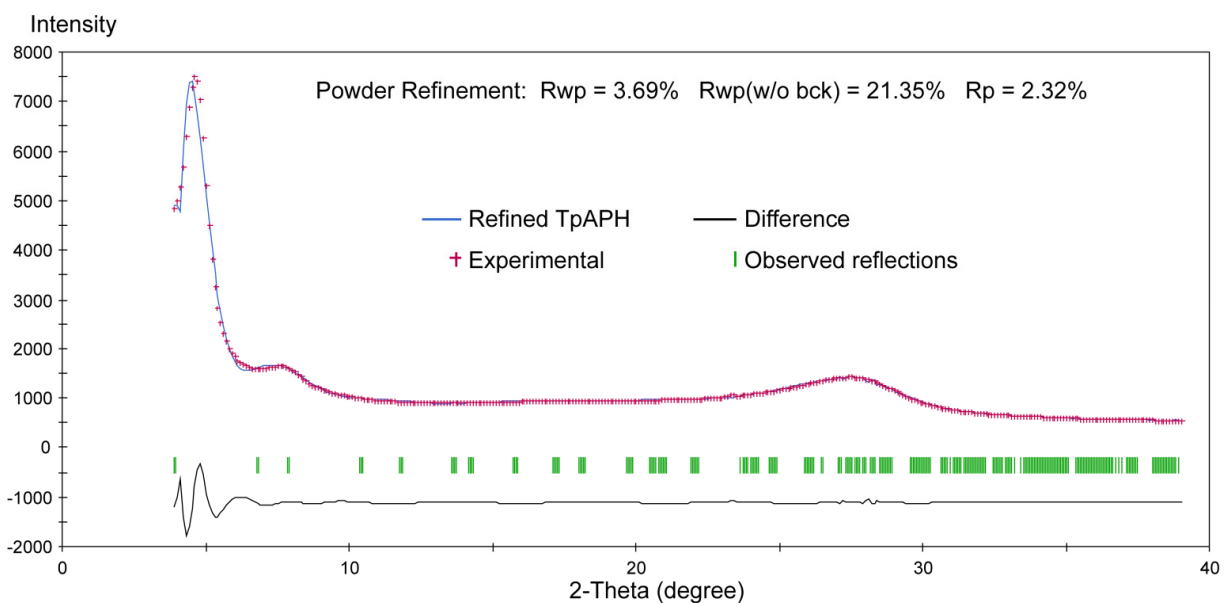


Figure S10. Comparison of PXRD pattern of experimental (crossed) and simulated (blue) TpAPH in eclipsed stacking mode. Difference plot is depicted in black line. Pawley refinement demonstrates good agreement between experimental and simulated eclipsed PXRD pattern (R_{wp} : 3.69%, R_p : 2.32%).

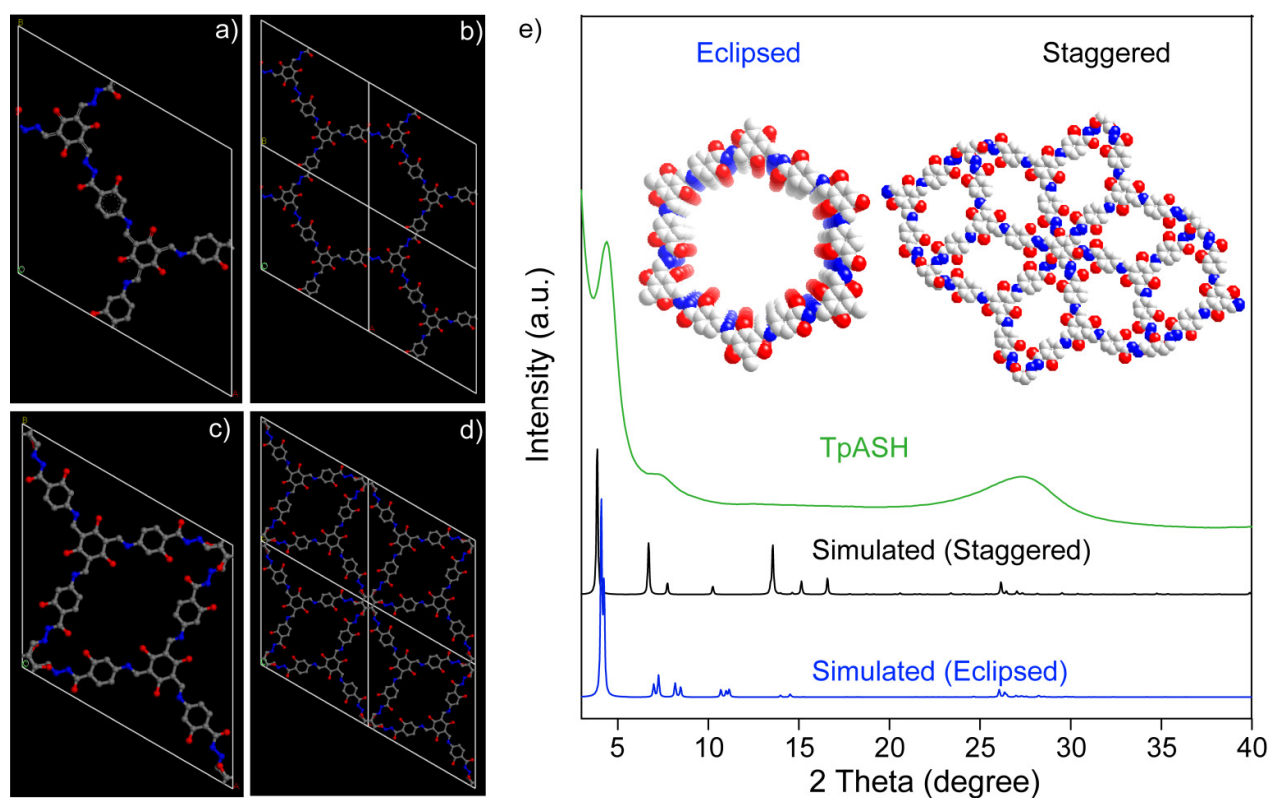


Figure S11. (a) Unit cell and (b) eclipsed crystal lattice packing of TpASH; (c) unit cell and (d) staggered crystal lattice packing of TpASH; (e) Comparison of PXRD patterns between TpASH experimental, staggered (simulated) and eclipsed (simulated). Inset indicate the space-fill modeling of TpASH COFs in eclipsed and staggered mode. Note: The crystallinity of these COFs reported in this paper are moderate, hence the model structures are approximate and hypothetical.

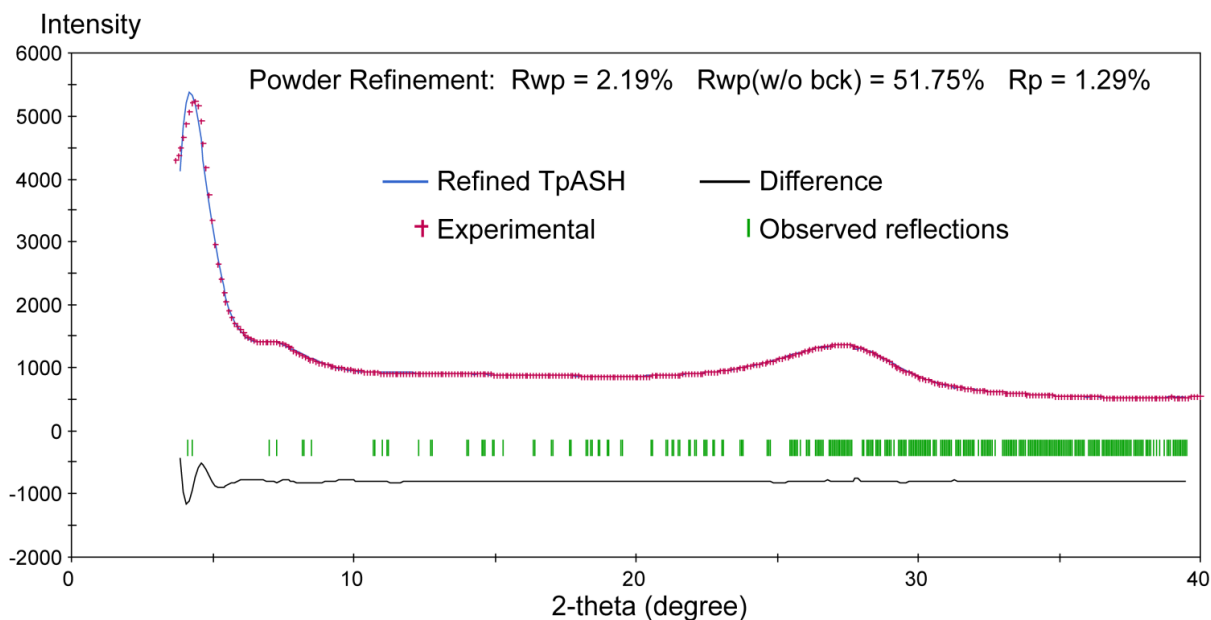


Figure S12. Comparison of PXRD pattern of experimental (crossed) and simulated (blue) TpASH in eclipsed stacking mode. Difference plot is depicted in black line. Pawley refinement demonstrates good agreement between experimental and simulated eclipsed PXRD pattern (R_{wp} : 2.19%, R_p : 1.29%).

Section S-5: Fractional atomic coordinates of unit cells

Table T1. Fractional atomic coordinates for unit cells of TpAPH.

TpAPH in eclipsed model			
<i>P1</i>			
$a = 25.9370, b = 26.0167, c = 3.4034 \text{ \AA}$			
Atom	x	y	z
C1	0.39366	0.51978	1.50459
N1	0.52265	0.46692	1.48047
N2	0.35999	0.59095	1.4916
C2	0.49613	0.54239	1.49535
N3	0.31646	0.60591	1.49566
C3	0.47759	0.48203	1.49445
C4	0.34489	0.53375	1.50441
C5	0.55547	0.39694	1.47716
C6	0.33306	0.66128	1.50614
C7	0.45474	0.56115	1.49909
C8	0.51014	0.41358	1.47539
C9	0.37638	0.45992	1.50631
O1	0.63555	0.4951	1.46066
O2	0.29176	0.49327	1.51211
C10	0.41686	0.44082	1.49823
C11	0.65821	0.42072	1.47723
C12	0.61686	0.4388	1.47171
C13	0.63955	0.36118	1.47852
C14	0.53868	0.33666	1.48522
C15	0.57977	0.31884	1.47776
C16	0.45416	0.03309	1.51226

N4	0.50884	0.21565	1.4912
C17	0.43251	0.11305	1.51919
C18	0.49316	0.15525	1.5034
C19	0.41314	0.05264	1.52234
C20	0.56245	0.25682	1.47339
C21	0.51433	0.07606	1.4993
C22	0.53402	0.1359	1.49166
C23	0.94819	0.59105	1.4835
N5	0.76414	0.45971	1.47937
C24	0.87096	0.48725	1.4983
C25	0.82681	0.50252	1.48701
C26	0.93098	0.53093	1.49532
C27	0.72163	0.47051	1.46571
C28	0.9033	0.60508	1.47512
C29	0.84383	0.56231	1.47354
N6	0.03075	0.592	1.52408
N7	0.08982	0.63539	1.51185
C30	-0.01226	0.60815	1.53401
C31	0.12863	0.61897	1.52541
C32	0.21333	0.72365	1.50686
O3	0.17895	0.74569	1.49942
C33	0.19148	0.66223	1.52327
C34	0.27417	0.76312	1.49911
C35	0.31332	0.74339	1.497
C36	0.23314	0.64376	1.52399
C37	0.29354	0.68371	1.51209
N8	0.37256	0.92424	1.48096
N9	0.3545	0.8649	1.49033
C38	0.43073	0.96495	1.48213
C39	0.2984	0.82757	1.51198
O57	0.67956	0.34635	0.48067
O4	0.48291	0.29757	0.50236
O5	0.21397	0.58727	0.53759
O6	0.36945	0.78225	0.48013

Table T2. Fractional atomic coordinates for unit cells of TpASH.

TpASH in eclipsed model			
<i>P1</i>			
a = 24.4087, b = 24.4173, c = 3.4153 Å			
Atom	x	y	z
C1	0.38436	0.50016	0.50725
N1	0.51388	0.44356	0.46754
N2	0.35105	0.57489	0.50316
C2	0.4859	0.52041	0.49098
N3	0.30775	0.59172	0.51227
C3	0.46953	0.46078	0.48665
C4	0.33702	0.51807	0.51255
C5	0.54745	0.37194	0.4556
C6	0.32328	0.64662	0.52582

C7	0.44388	0.53998	0.49989
C8	0.50235	0.39053	0.45917
C9	0.36924	0.441	0.50545
O1	0.62508	0.46716	0.4402
O2	0.28512	0.47964	0.52154
C10	0.41036	0.42112	0.49225
C11	0.64867	0.39154	0.44858
C12	0.60749	0.4114	0.44821
C13	0.63118	0.33252	0.4466
C14	0.5318	0.3121	0.46013
C15	0.57272	0.2925	0.4476
O3	0.4609	0.59876	0.50261
C16	0.44528	0.01206	0.47031
N4	0.50424	0.19183	0.4587
C17	0.4226	0.09327	0.48573
C18	0.4819	0.13311	0.46814
C19	0.4044	0.03341	0.48557
C20	0.55659	0.23094	0.43965
C21	0.5041	0.05272	0.45567
C22	0.52262	0.11198	0.45125
O4	0.3459	-0.00502	0.50161
C23	0.92192	0.56069	0.44528
N5	0.75281	0.42627	0.44462
C24	0.8531	0.45757	0.45748
C25	0.80612	0.47027	0.45134
C26	0.91037	0.50219	0.45323
C27	0.71061	0.43889	0.43563
C28	0.8743	0.57215	0.44199
C29	0.81751	0.52843	0.44173
O5	0.95592	0.48876	0.45799
N6	0.02543	0.58965	0.56456
N7	0.08316	0.63077	0.55075
C30	-0.01736	0.60765	0.57957
C31	0.1218	0.61264	0.5595
O6	-0.0042	0.65918	0.57385
C32	0.20388	0.71424	0.54221
O7	0.16954	0.73781	0.53964
C33	0.18326	0.65348	0.55541
C34	0.26343	0.75133	0.5324
C35	0.30244	0.7299	0.52523
C36	0.22476	0.63319	0.55095
C37	0.28386	0.67079	0.53707
N8	0.35816	0.90901	0.51896
N9	0.34126	0.85018	0.525
C38	0.41505	0.94746	0.51838
C39	0.28636	0.81504	0.54841
O8	0.67097	0.31597	0.44714
O9	0.47728	0.27517	0.482
O10	0.2067	0.57726	0.56466
O11	0.35735	0.76658	0.50982

Section S-6: Characterization details of the two COFs

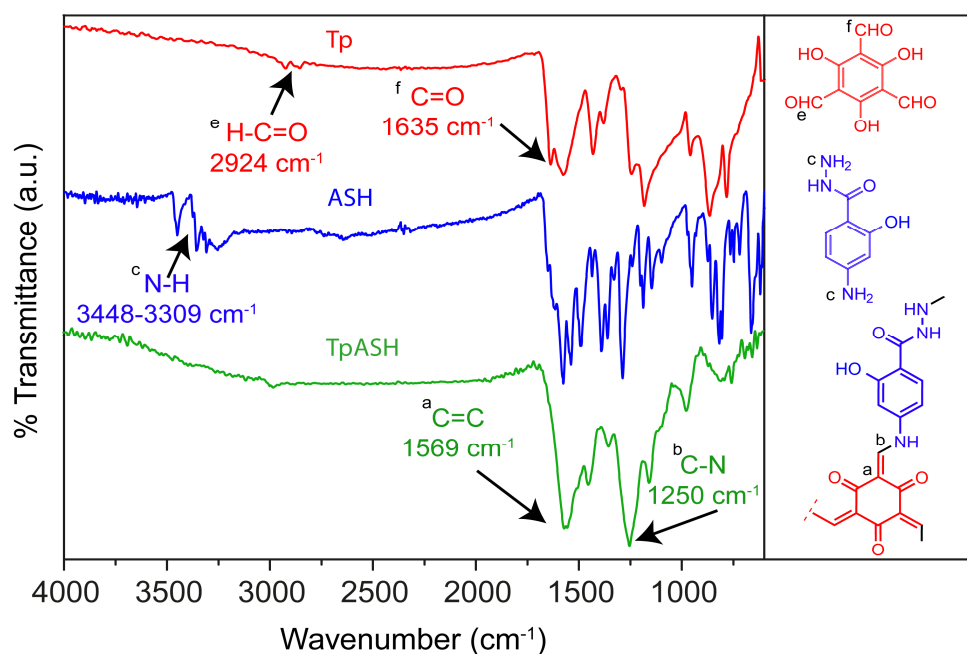


Figure S13. Comparison of FTIR spectra between Tp, ASH and TpASH.

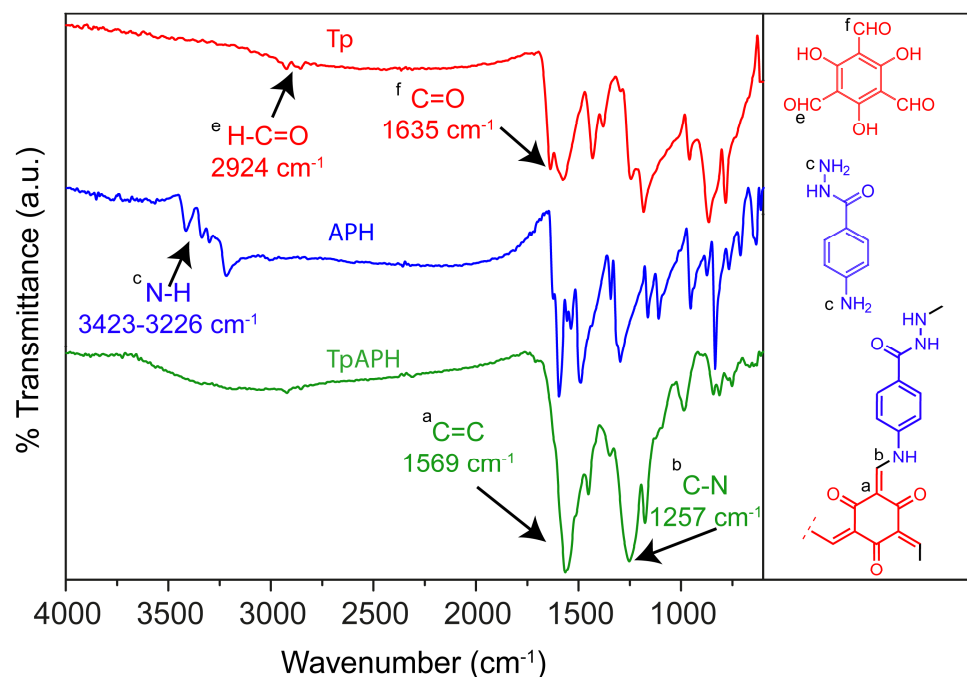


Figure S14. Comparison of FTIR spectra between Tp, APH and TpAPH. Both the FTIR spectra revealed the formation of COFs from the subsequent diamines. Characteristic carbonyl ($-\text{C}=\text{O}$) stretching frequency at 1635 cm^{-1} , $\text{C}-\text{H}$ stretching frequency (2924 cm^{-1}) of the aldehyde in Tp and $\text{N}-\text{H}$ stretching frequency ($3448-3226 \text{ cm}^{-1}$) of primary amine was disappeared in the corresponding product. This suggested complete utilization of the starting materials to form the product. Meanwhile in a characteristic $\text{C}=\text{C}$ stretching frequency was observed at 1569 cm^{-1} and the characteristic stretching at $1250-1257 \text{ cm}^{-1}$ was assigned to $\text{C}-\text{N}$ stretching frequency.

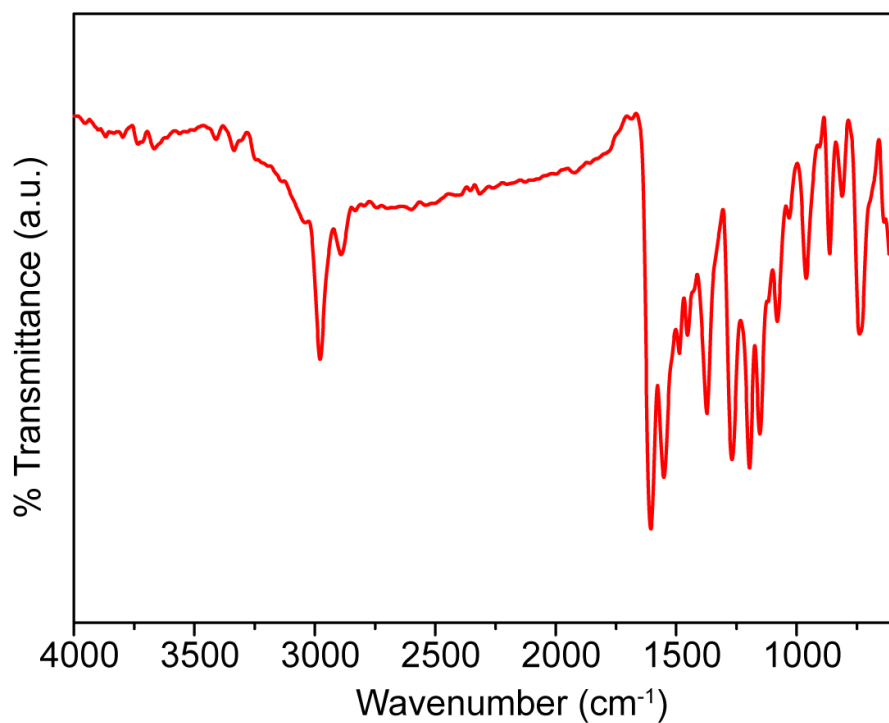


Figure S15. FTIR spectra of TpASH monomer. A characteristic C=N stretching frequency is observed at 1606 cm^{-1} , since enol to keto tautomerism is not possible in the monomer.

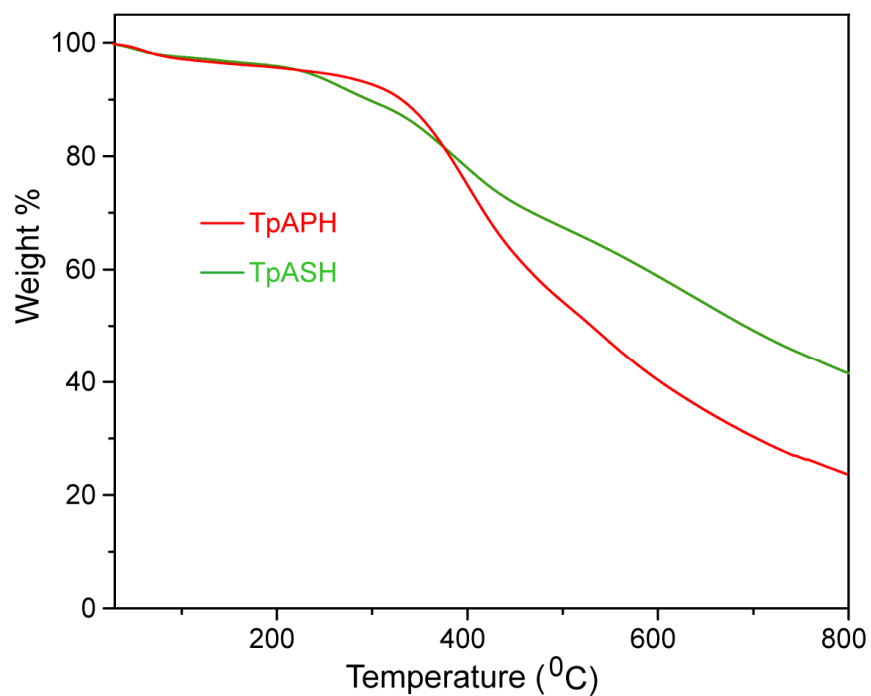


Figure S16. TGA profiles of activated TpAPH and TpASH. Both the COFs show thermal stability up to $300\text{ }^{\circ}\text{C}$.

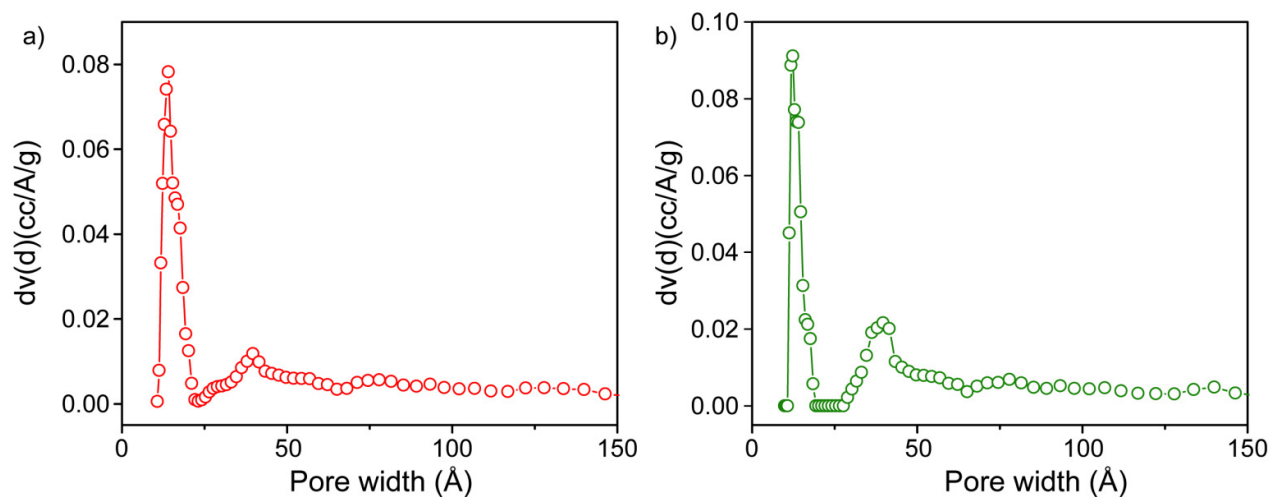


Figure S17. Pore size distribution of (a) TpAPH and (b) TpASH respectively; where TpAPH shows pore diameter of 14Å and TpASH shows pore diameter of 13Å which is as expected.

Section S-7: Morphological analysis of the COFs

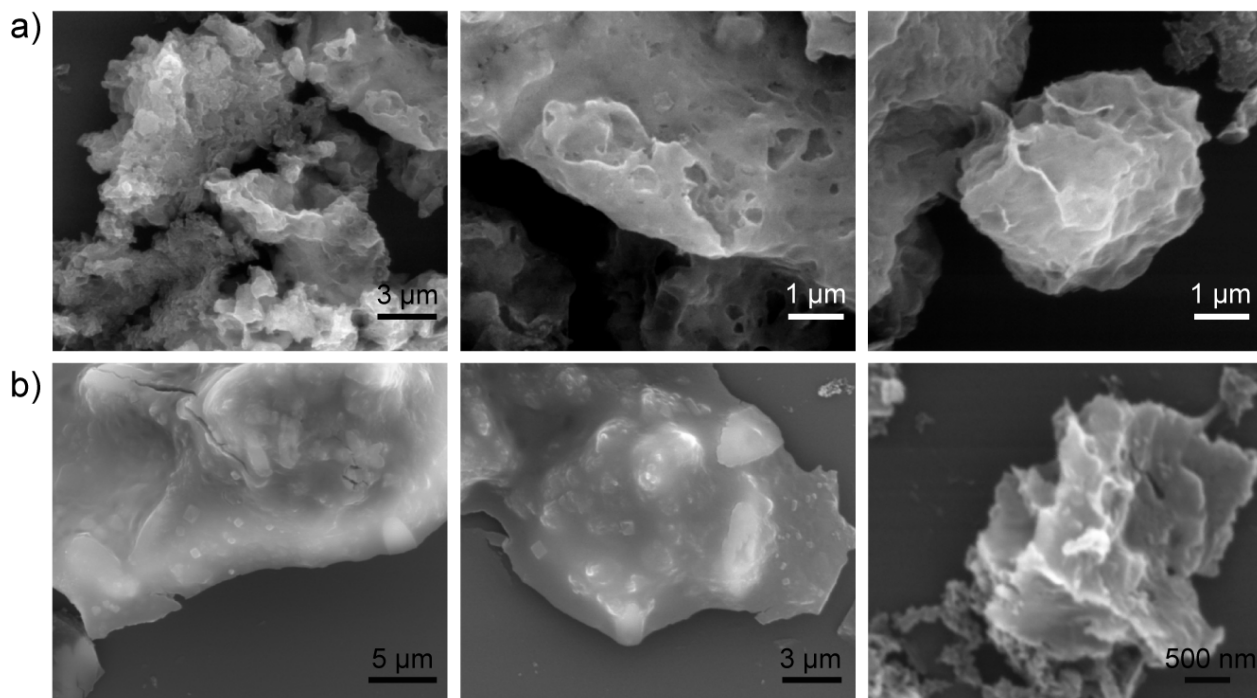


Figure S18. SEM images of (a) TpAPH and (b) TpASH, which demonstrated assembly of sheet like morphology.

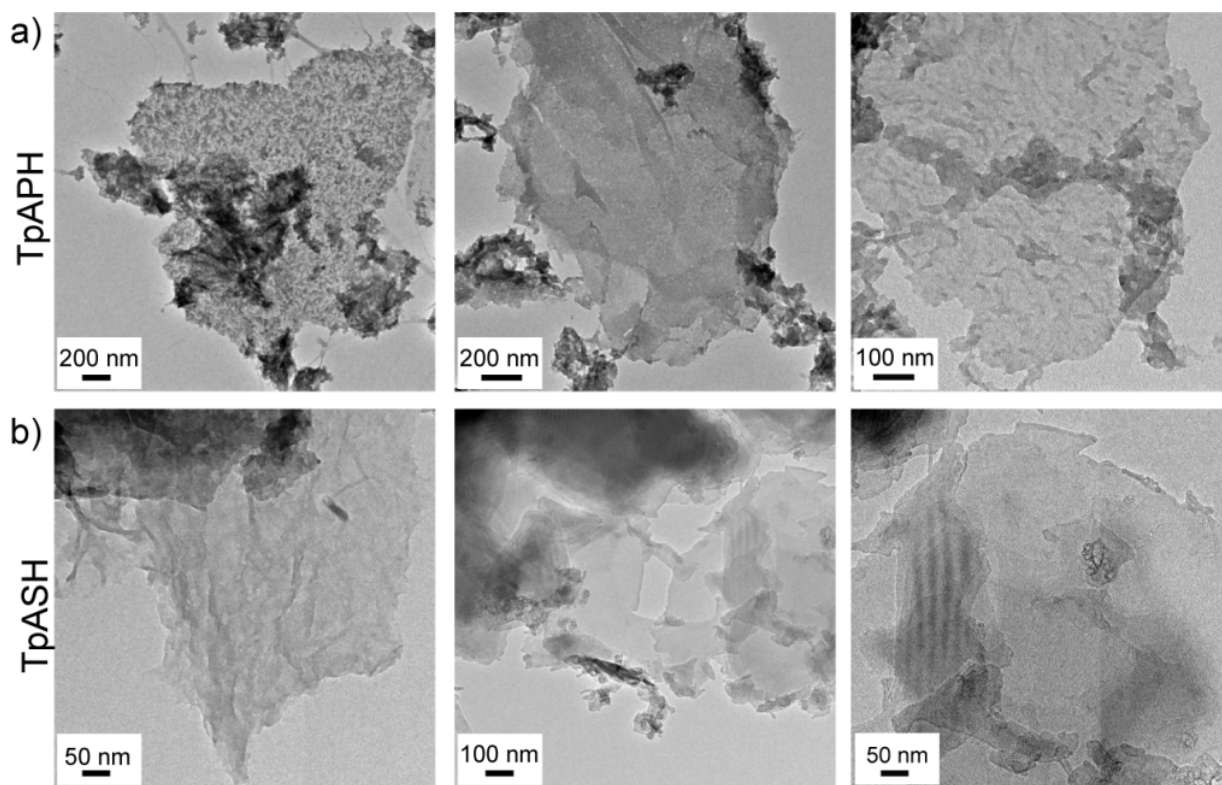


Figure S19. TEM images of (a) TpAPH and (b) TpASH, which demonstrated assembly of thin, transparent sheet like morphology.

Section S-8: Stability study of TpASH

We have used TpASH for further fabrication steps to devise a CONS-based targeted drug delivery system utilizing the hydroxyl group present within the framework. Prior to fabrication, we have checked the aqueous stability of TpASH using FTIR and PXRD analysis. TpASH was submerged in aqueous medium for about 10 days, then the sample was centrifuged, dried and subjected to FTIR and PXRD analysis. No alterations in both the study demonstrate the stability of TpASH in aqueous medium.

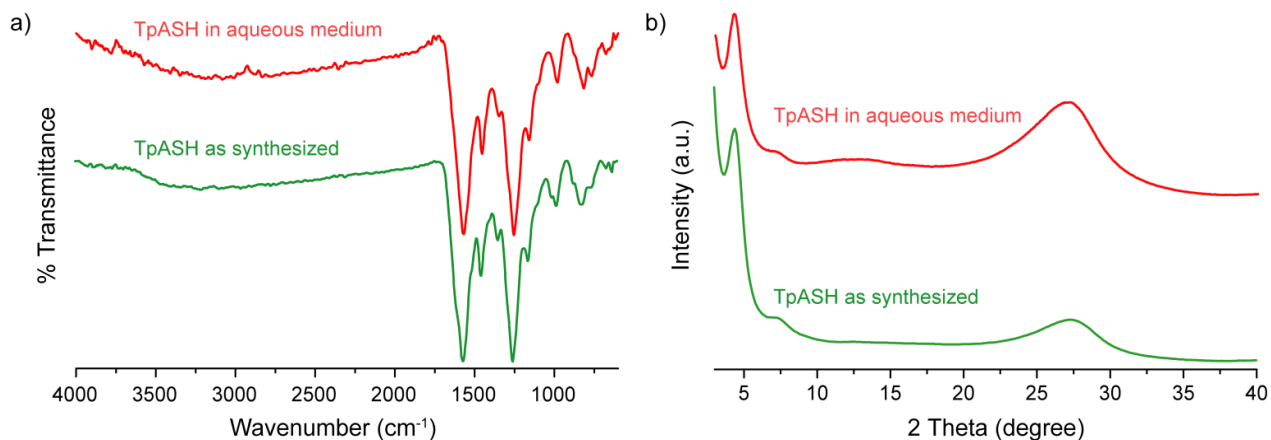


Figure S20. Stability study of TpASH in aqueous medium, (a) comparison of FTIR spectra (b) comparison of PXRD pattern. Both the study shows that TpASH is stable in aqueous medium.

Section S-9: COF to functionalized CONs *via* postsynthetic modification steps

Synthesis of TpASH-Glc CONs: 60 mg of purified TpASH COF was dispersed in 25 mL of 0.1M NaHCO₃ solution for about 5 min by sonication in a water bath. To it 750 μ L of glycidol (Glc) was added and the reaction mixture was kept under reflux for 24 h. After the reaction was complete the reaction mixture was allowed to cool down to room temperature. The TpASH-Glc CONs was separated by centrifugation at 6000 rpm for about 6 min, washed with EtOH and dried at 60 °C for overnight.

Synthesis of TpASH-APTES CONs: 50 mg of TpASH-Glc CONs was dispersed in 25 mL of toluene by sonication under N₂ atmosphere. To it 500 μ L of 3-aminopropyltriethoxy silane (APTES) was added and the reaction mixture was refluxed under N₂ atmosphere for overnight. The product was separated by centrifugation followed by washing with EtOH (3 times). Finally the product was dried at 60 °C for overnight. For TpAPH similar methodology was used for APTES conjugation. The product was dried at 60 °C and 90 °C for overnight.⁷

Synthesis of TpASH-FA CONs: 15 mg of folic acid (FA) was dissolved in 15 mL of aq. DMSO (1:1) by sonication. To it 3-5 mg of EDC.HCl and 3-5 mg of NHS was added and pH was maintained at pH 6-7. Activation of FA was carried out for 3 h under dark condition. To this activated FA, 15 mg of TpASH-APTES CONs (dispersed in 3 mL water) was added dropwise. 2-3 drops of pyridine was added to it and the pH was maintained at pH 7.5-8. This reaction mixture was stirred for overnight under dark. Finally the product was centrifuged, washed with aq. DMSO, water, EtOH and dried at 60 °C for overnight.⁷

Surface accessible amine quantification by *p*-nitrobenzaldehyde assay: Surface accessible amine was quantified by *p*-nitrobenzaldehyde assay reported by Bruce et al.⁸ Briefly, 5 mg of CONs sample (TpASH-APTES and TpASH-FA) was placed in a 1.5 mL eppendorf tube. To it, 1 mL of *p*-nitrobenzaldehyde solution (7 mg in 10 mL of coupling buffer) was added, and it was allowed to react for 3 h with gentle end to end rotation. After the removal of the supernatant followed by washings, 1 mL of hydrolysis solution (75 mL of H₂O, 75 mL MeOH and 0.2 mL glacial acetic acid) was added to the CONs sample. It was shaken further for an hour. The supernatant was removed and the absorbance was measured at 282 nm. From UV-Vis spectrophotometric study surface accessible amine was quantified against a standard solution of *p*-nitrobenzaldehyde. *Note:* Although *p*-nitrobenzaldehyde assay was used for accessible amine quantification, but this process is very qualitative for CONs.

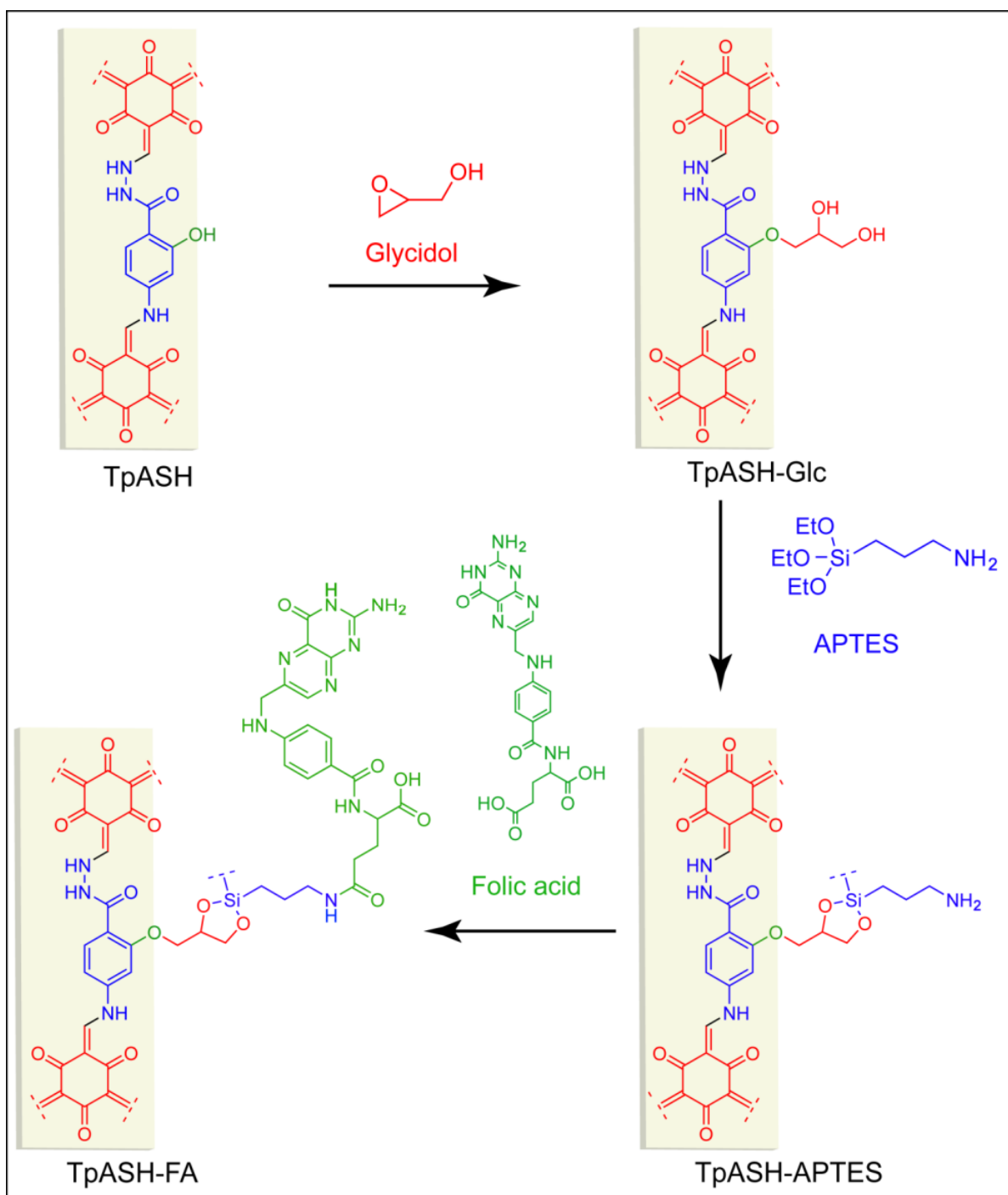


Figure S21. Schematic representation of the respective chemical structures of sequential postsynthetic modification steps. Change in functionality has been denoted using a single hydroxyl group; however two subsequent hydroxyl groups can participate in the reaction.

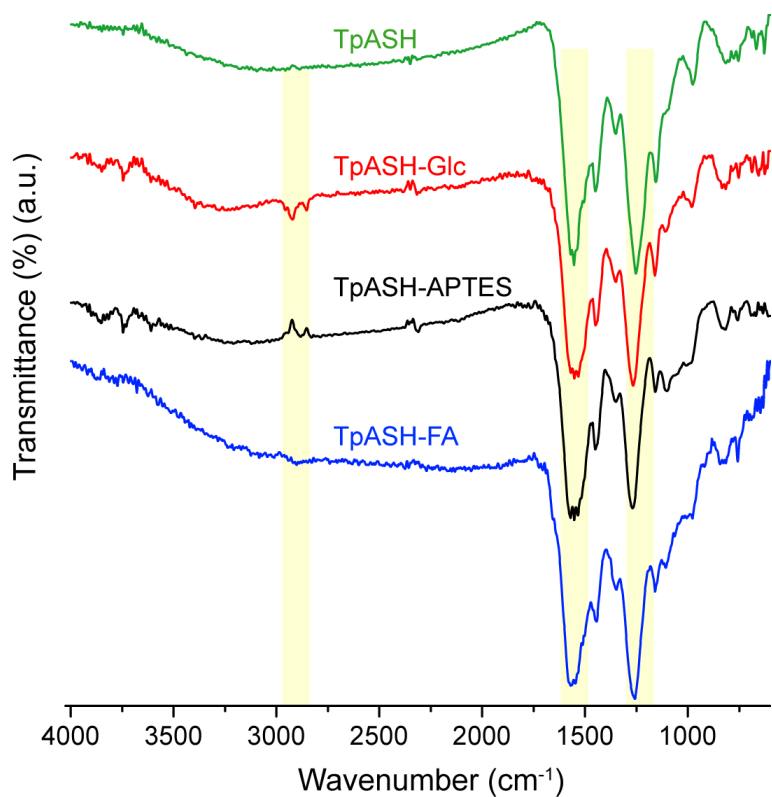


Figure S22. Comparison of FTIR spectra between the as synthesized TpASH and sequential functionalized steps to functionalized CONs.

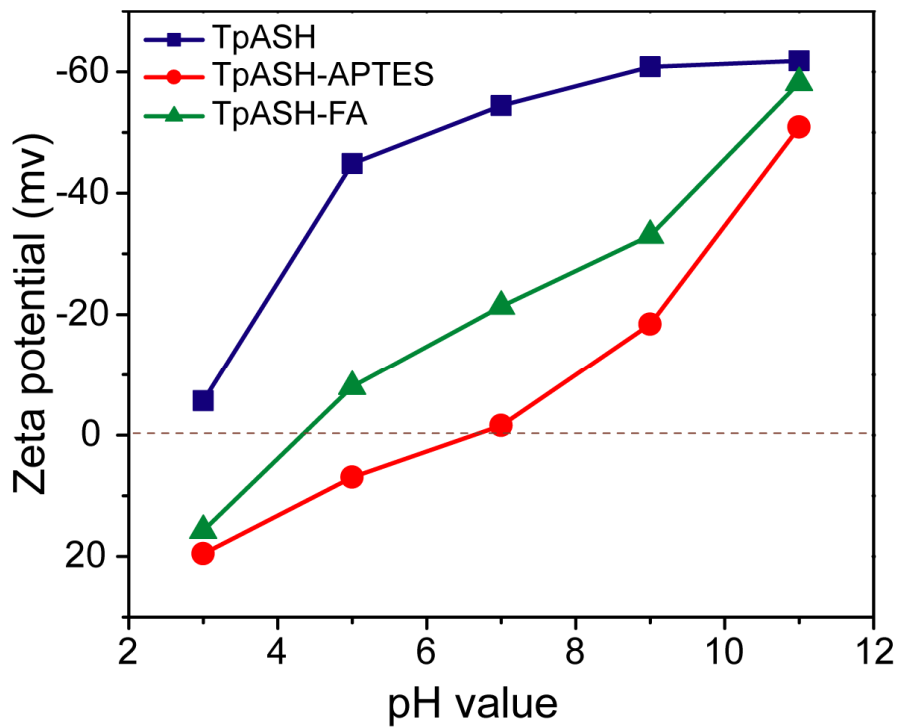


Figure S23. Comparison of zeta potential between TpASH, TpASH-APTES and TpASH-FA.

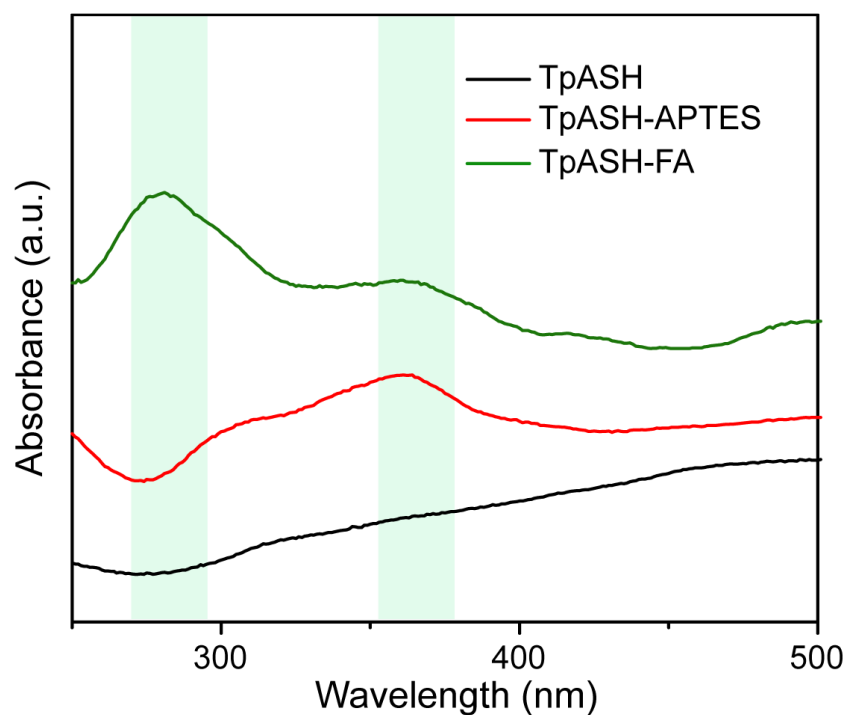


Figure S24. Comparison of UV-Vis spectra between TpASH, TpASH-APTES and TpASH-FA.

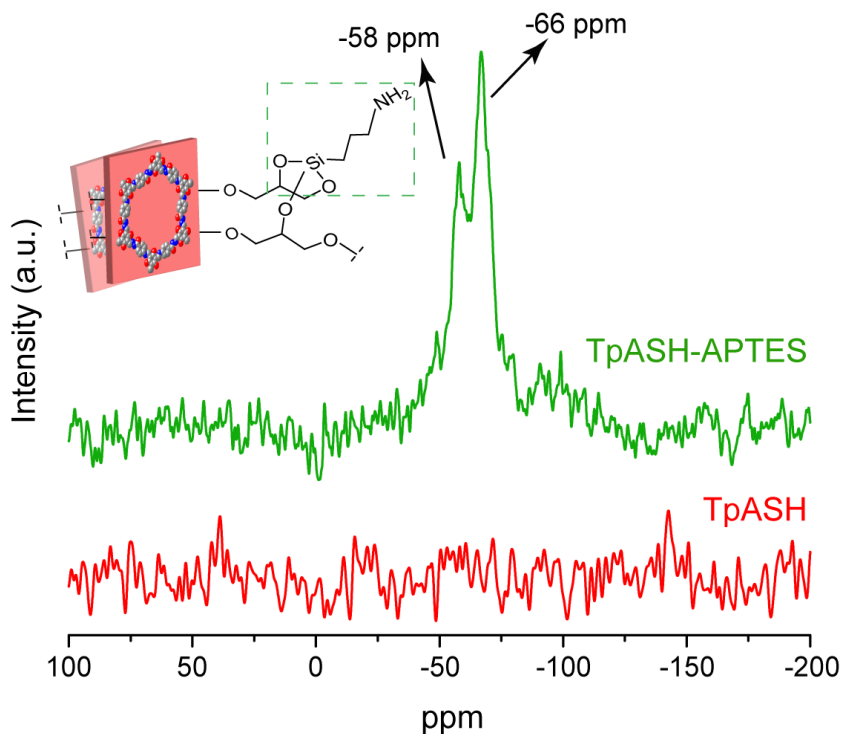


Figure S25. Comparison of ^{29}Si CP MAS solid state NMR of TpASH and TpASH-APTES CONs; where pristine TpASH is ^{29}Si CP MAS solid state NMR silent, but TpASH-APTES CONs show characteristic Si signal signifying successful conjugation of APTES.

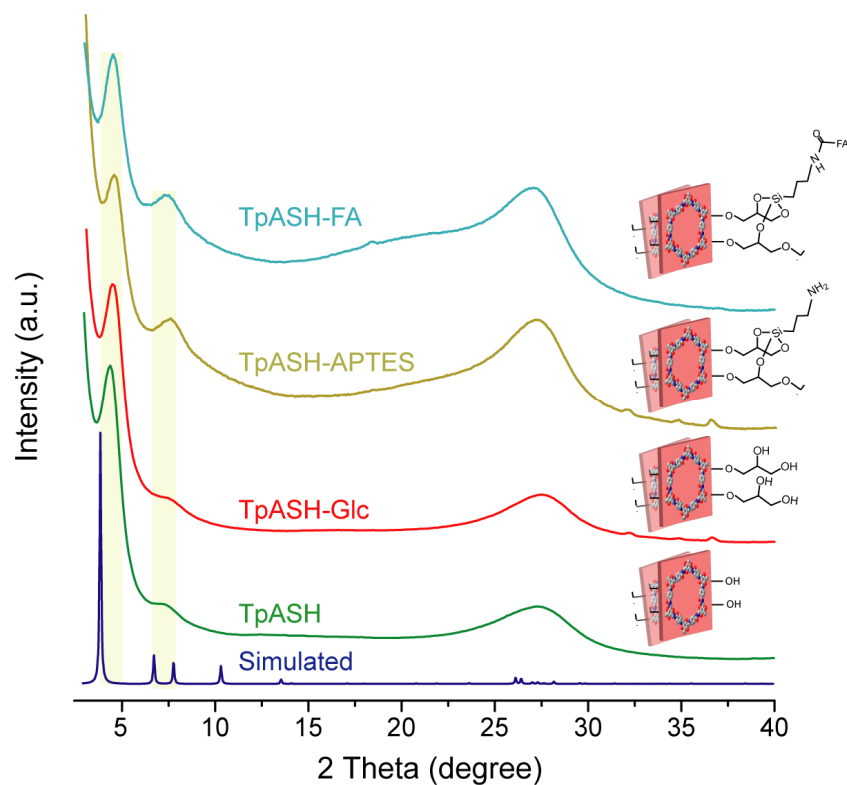


Figure S26. Comparison of PXRD pattern between the as synthesized TpASH and functionalized targeted CONs. The first peak in PXRD pattern is retained after postsynthetic modification signifying its structural integrity.

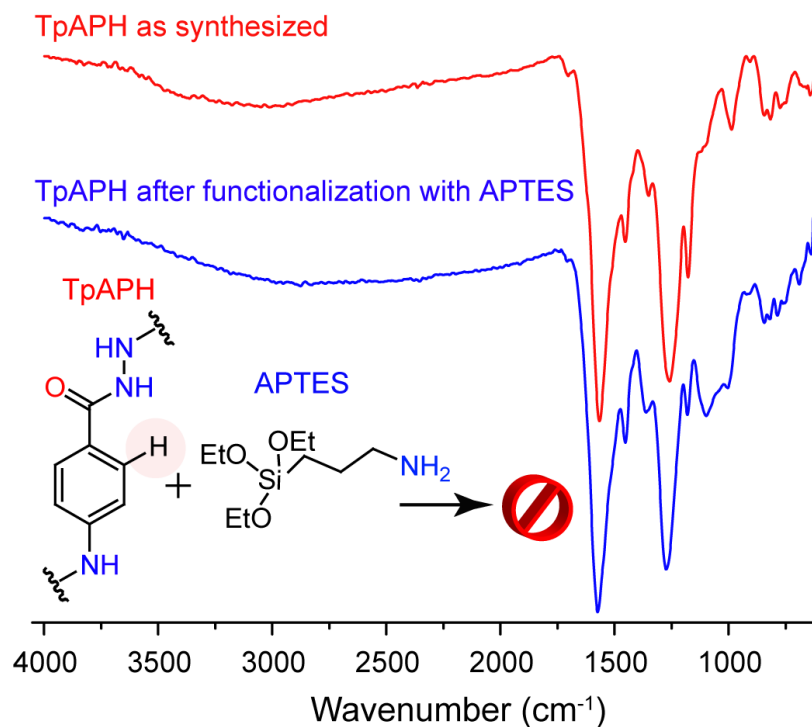


Figure S27. Comparison of FTIR spectra of TpAPH after reaction with APTES and as synthesized TpAPH. Due to the absence of hydroxyl groups amine functionalization is not possible here. However, slight possibility of self-condensation of APTES could not be ruled out.

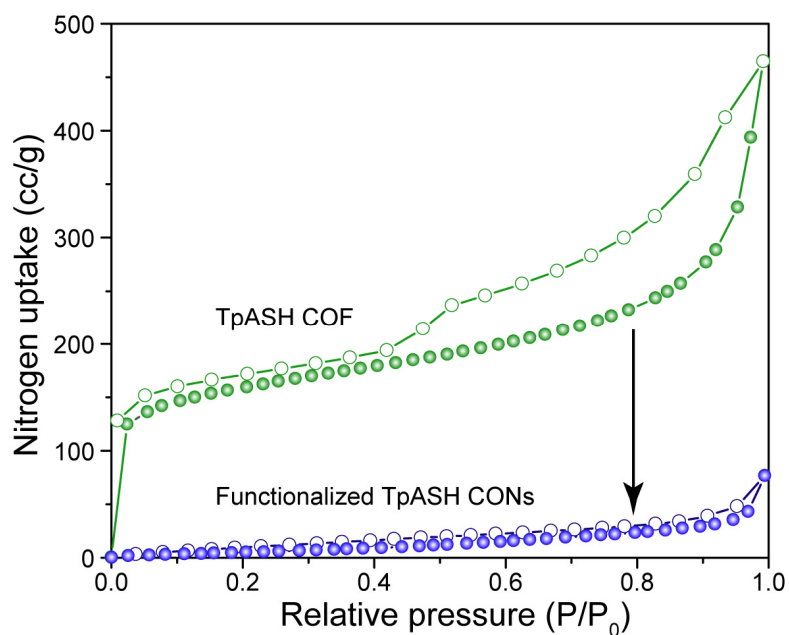


Figure S28. Comparison of BET surface area between COF and functionalized CONs. A sharp reduction in surface area signified exfoliation phenomenon after postsynthetic modifications.

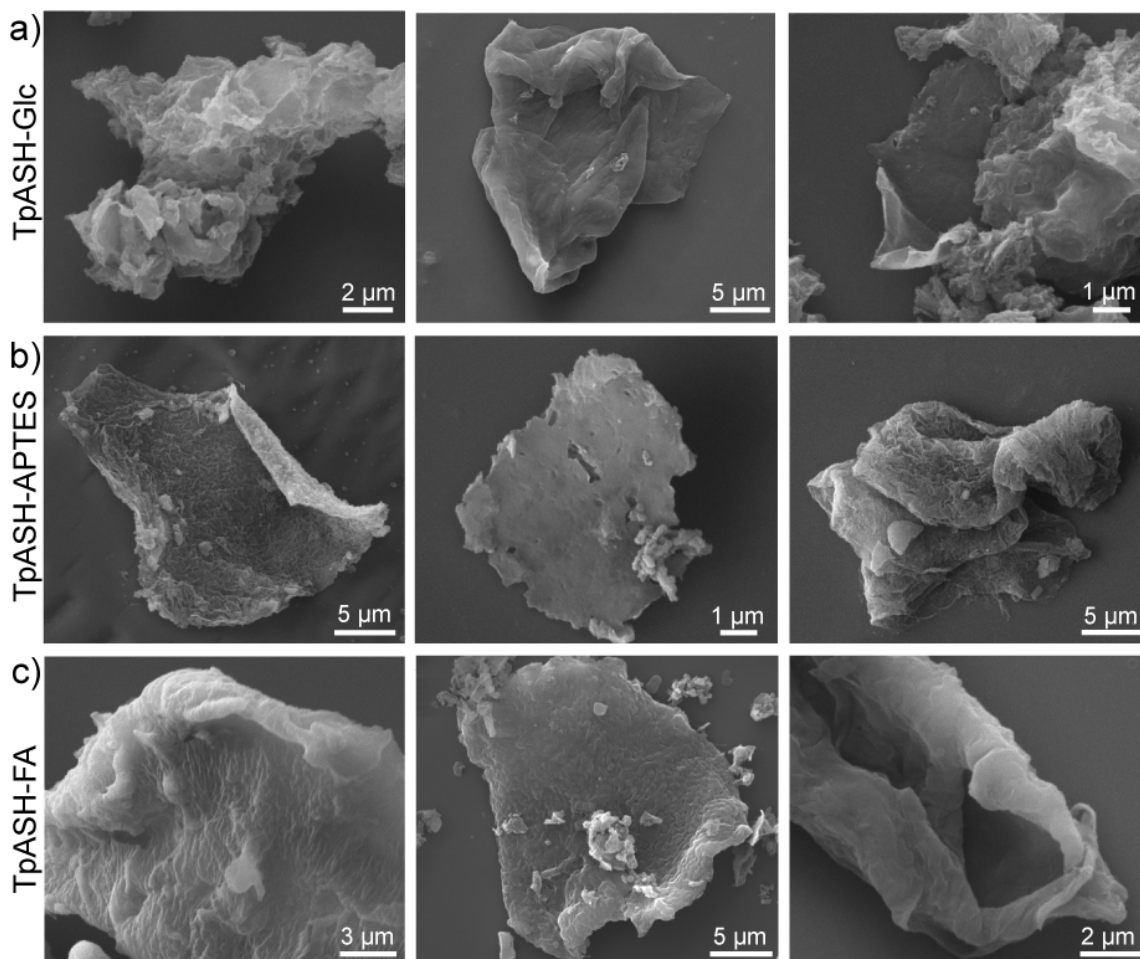


Figure S29. SEM images of functionalized CONs (a) TpASH-Glc, (b) TpASH-APTES and (c) TpASH-FA.

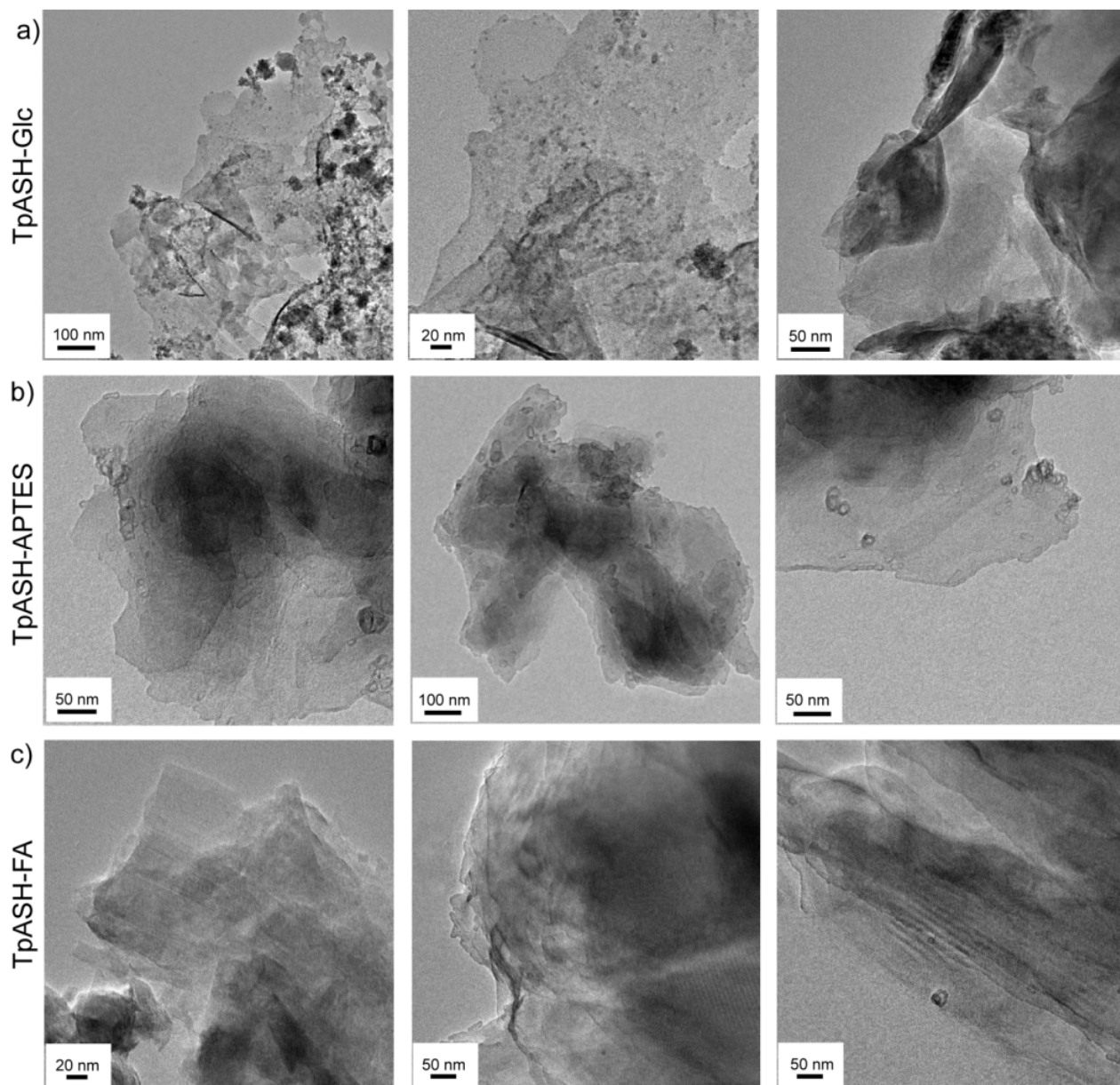


Figure S30. TEM images of functionalized exfoliated CONs (a) TpASH-Glc, (b) TpASH-APTES and (b) TpASH-FA.

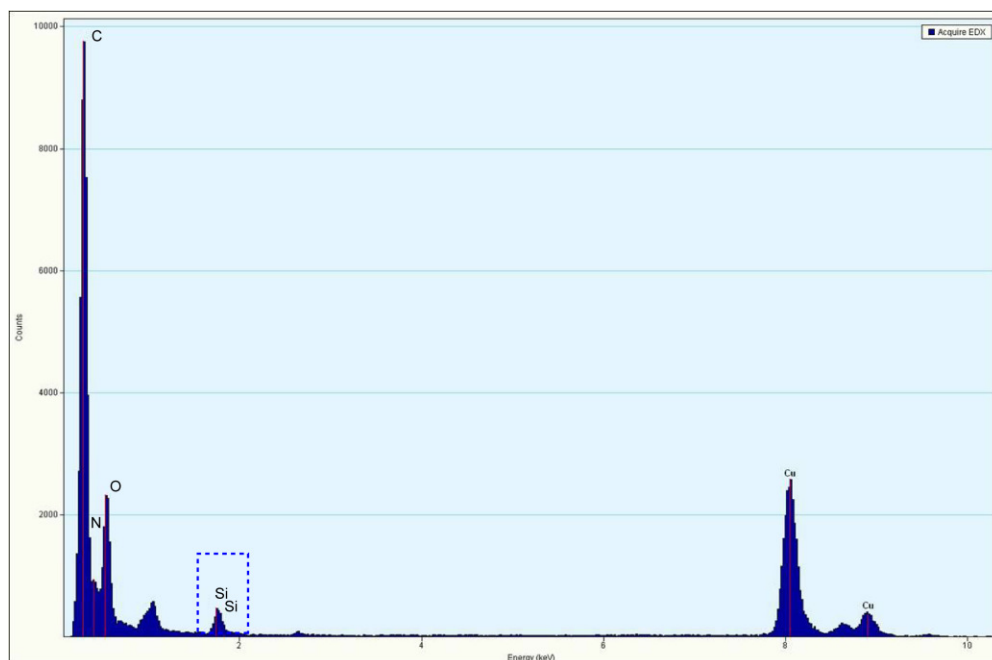


Figure S31. EDX analysis of TpASH-APTES. It shows the presence of C, N, O and Si which is consistent with experimental result as well.

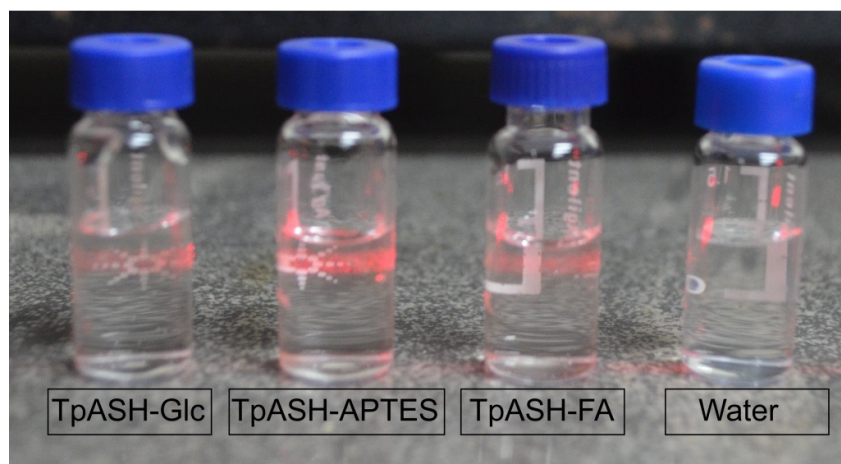


Figure S32. Aqueous dispersion of CONs: (i) TpASH-Glc, (ii) TpASH-APTES, (iii) TpASH-FA in water. All the three CONs exhibited Tyndall Effect signifying stable dispersion. Source of laser light is from right hand side.

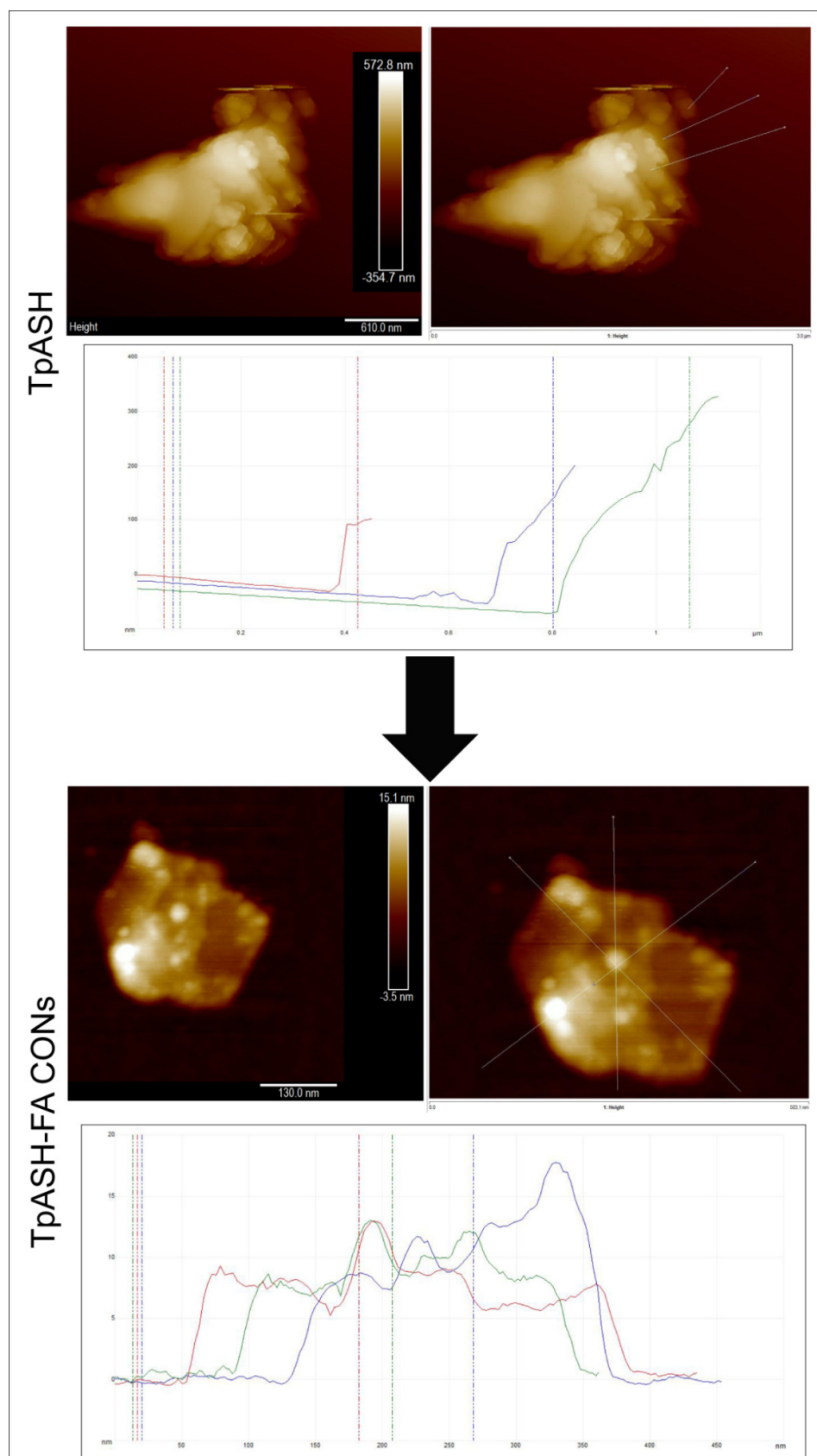


Figure S33. Comparison of average height profile between COF and functionalized postsynthetically modified CONS as observed by AFM.

Section S-10: Detailed biological studies

Drug loading: Anticancer drug 5-fluorouracil (5-FU) was loaded on to TpASH-FA CONs. About 10 mg of 5-FU was dissolved in 5 mL of water; to it 20 mg of TpASH-FA CONs dispersed in 5 mL of water was added slowly. The mixture was stirred for 6 h at room temperature, followed by centrifugation at 6000 rpm. Drug loaded sample was washed with water to remove the physically adsorbed 5-FU. Drug loading was evaluated UV-Vis spectrophotometrically by measuring the absorbance at 280 nm of a standard 5-FU solution and supernatant respectively.⁷

Drug release: Cumulative release of 5-FU from TpASH-FA-5FU was studied at two different pH; pH 5 which was comparable to intracellular lysosomal pH of cancer cells and pH 7.4 the extracellular pathophysiological pH of normal cells. Briefly, 3 mg of TpASH-FA-5FU was dispersed in 3 mL of buffer solution and sealed inside a dialysis bag (molecular cut off 50 kDa). It was then immersed in 100 mL of external buffer medium kept in a bowl. Dialysis was continued at 37 °C and drug release was monitored UV-Vis spectrophotometrically by measuring the absorbance of the external buffer at 280 nm (against a standard solution).⁷

Fluorescent conjugation: TpASH-FA CONs of appropriate concentration was dispersed in 0.1 M NaHCO₃ solution. To it, 1 mg of RITC dissolved in 2 mL of aqueous DMSO (1 : 1, v/v) was added instantly and the reaction mixture was stirred at room temperature for 24 h in a dark condition. RITC labelled folate targeted TpASH CONs (TpASH-FA-RITC) was separated by centrifugation at 6000 rpm. TpASH-FA-RITC was washed and redispersed in water repeatedly to remove excess of RITC. TpASH-APTES was labeled with RITC (TpASH-APTES-RITC) using the same procedure and was used in control CONs set.⁷

MTT assay: Breast cancer cell lines (MDA-MB-231) were purchased from NCCS, Pune. These cells were accessed for *in vitro* toxicity study by MTT [3-(4, 5-dimethylthiazol-2-yl)-2,5-diphenyltetrazolium bromide] assay following standard procedures. All the cultures were maintained in a phenol red free culture medium containing DMEM/F12 (Dulbecco's modified essential medium/Ham's 12 nutrient mixture, Gibco), supplemented with 5% (v/v) fetal calf serum (JS Bioscience, Australia), and 1% (v/v) antibiotic (2 mM L-glutamine, 100 U/mL Penicillin and 0.1 mg/mL Streptomycin; Gibco). Cultured cells were kept at 37 °C in a humidified 5% CO₂ incubator. The cells were seeded in a 96 well plates and allowed to adhere for 24 h. After this time, they were incubated for 48 h with different concentrations of TpASH, TpASH-APTES-5FU and TpASH-FA-5FU respectively followed by incubation in media containing 0.5 mg/mL of MTT for 3-4 h at 37°C. The resulting formazan crystals

were dissolved in an MTT solubilization buffer and the absorbance measured at $\lambda = 570$ nm by using a microplate reader (Biorad). The obtained values were compared to the control cells.⁷

Cellular uptake study: Human breast cancer cells (MDA-MB-231) were chosen for cellular uptake study, cells with density of 2×10^4 cells per well were seeded into 24 well culture plate. After 24 h interval culture medium was removed and fresh medium with TpASH-FA-RITC CONs was added in each well. Intracellular localization of TpASH-FA-RITC CONs was observed on human breast cancer cells (MDA-MB-231) under fluorescent microscopy. Cells were fixed by using 4% formaldehyde for 15 min. The samples were washed by PBS and then treated with 0.1% Triton-X for permeabilisation of membrane. After that 1% bovine serum albumin (BSA) was added; followed by staining the cells nuclei by DAPI for 30 min and imaged by fluorescent microscopy. In contrast, non-targeted CONs (TpASH-APTES-RITC) was used as control against the same MDA-MB-231 cells.^{7,9}

Cellular migration assay: Breast cancer cell line MDA-MB-231 was maintained following standard protocol. Migration was measured by wound healing assay, in which cells were grown to 80% confluence in 6-well plates, streaked with a sterile pipette tip, and allowed to recover in media. After 24 h, plates were visualized under inverted microscope and migration determined by measuring wound width using the image J software. Control and drug loaded targeted CONs (TpASH-FA-5FU) were used in this study.

Microscopic study for apoptosis assay: Human breast cancer cells (MDA-MB-231) were chosen for apoptosis study, cells with density of 2×10^4 cells per well were seeded into 24 well culture plate. After 24 h interval culture medium was removed and fresh medium with TpASH-APTES-5FU and TpASH-FA-5FU CONs was added in each well. And the cells were allowed to incubate for further 24 h. Cells were then fixed by using 4% formaldehyde for 15 min and the samples were washed by PBS buffer. The fixed cells were then observed under inverted microscope. In contrast, under similar condition MDA-MB-231 cells were used as the control sets.⁹ Control cells are expected to retain their morphology after this study whereas the cells inducing apoptosis are expected to demonstrate fragmentation within the nucleus.

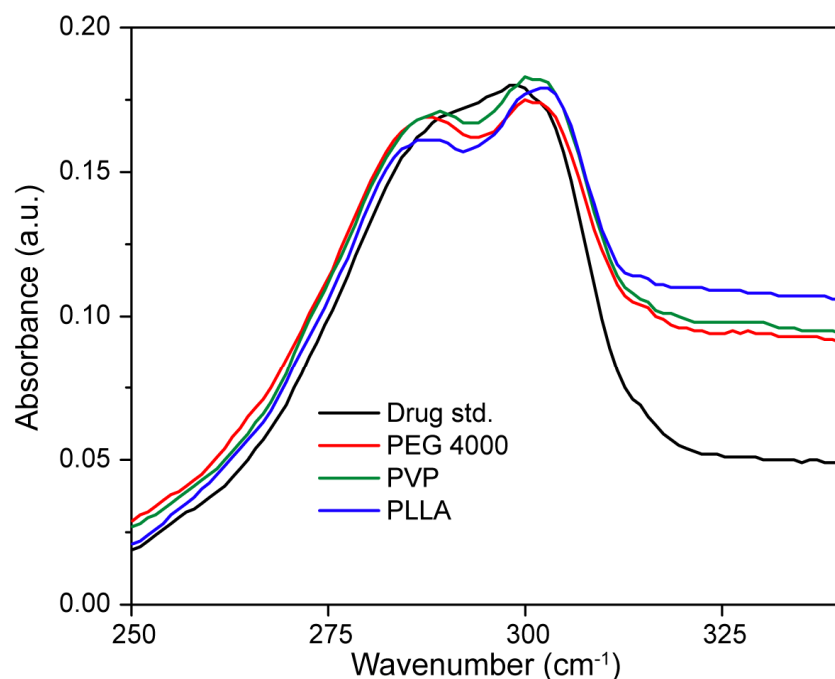


Figure S34. Comparison of drug loading using biocompatible polymers: polyethylene glycol-4000 (PEG-4000), polyvinylpyrrolidone (PVP), polylactic acid (PLLA). Maximum of ~5% loading of 5-FU was noted which was less compared to the targeted CONs (where ~12% loading was noted considering its porous structure, but regular/periodic porosities are absent in aforementioned biocompatible polymers). Same amount of polymers were used during the loading experiment.

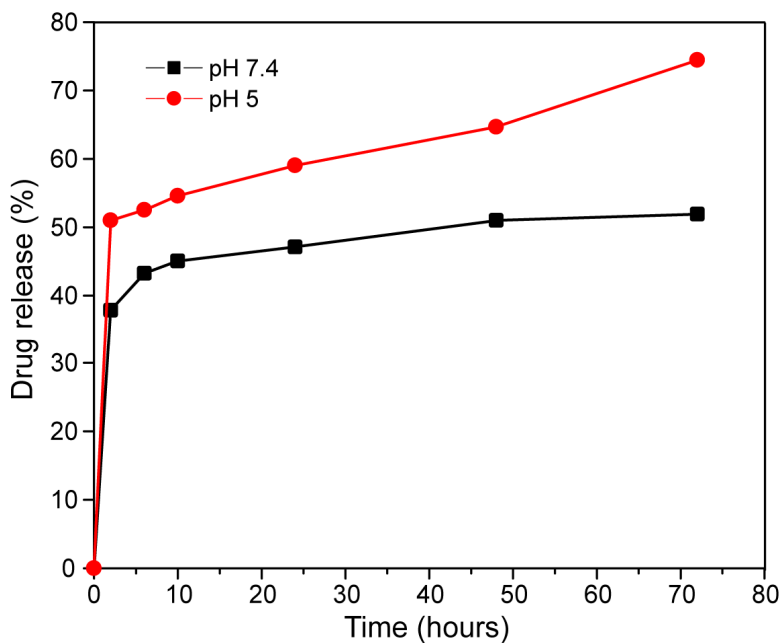


Figure S35. Release pattern of 5-FU from TpASH-FA-5FU at two different pH (pH 5 and pH 7.4) under mimicking environment. At acidic pH 5 preferential sustained release of 5-FU was noted for about 72 h compared to physiological pH 7.4 (where 50% loaded 5FU was released after 72 h). Therefore, this could establish a cancer specific drug release with minimum release in normal cells.

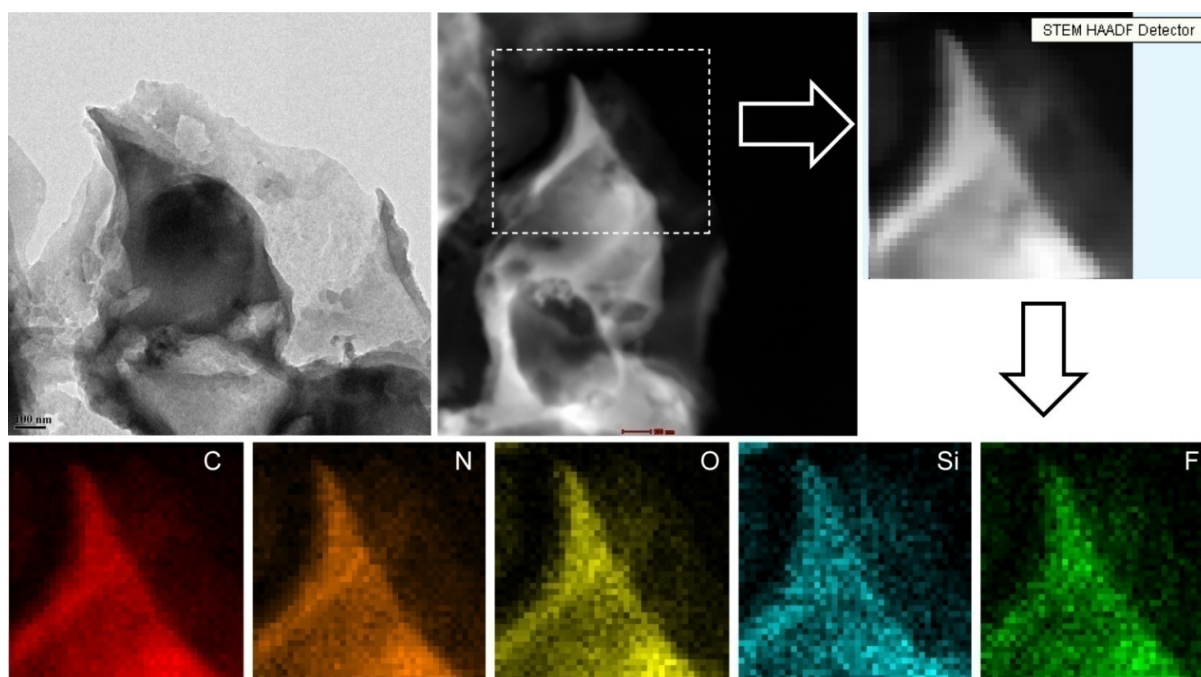


Figure S36. STEM-HAADF elemental mapping of TpASH-FA-5FU. Mapping analysis shows presence of C, N, O, Si and F as the major constituents of the drug loaded sample which is also consistent with the experimental result. In our UV-Vis study we ensured 12% loading of 5-FU on to TpASH-FA. Additionally we also evaluated false drug loading experiment. Hence after drug loading and washing we further stirred the sample with 5-FU. Interestingly no significant change in the UV-Vis pattern was noted. This could be a fare evidence that the drug was loaded on to the CONs.

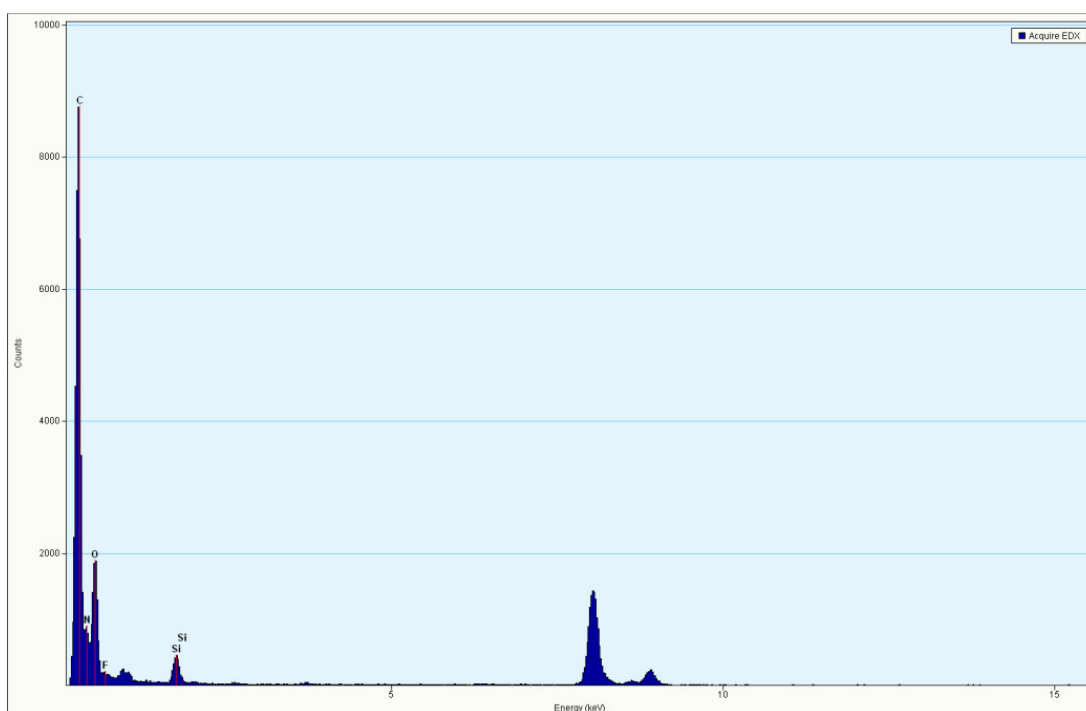


Figure S37. EDX analysis shows presence of C, N, O, Si and F as the major constituents of the drug loaded CONs sample.

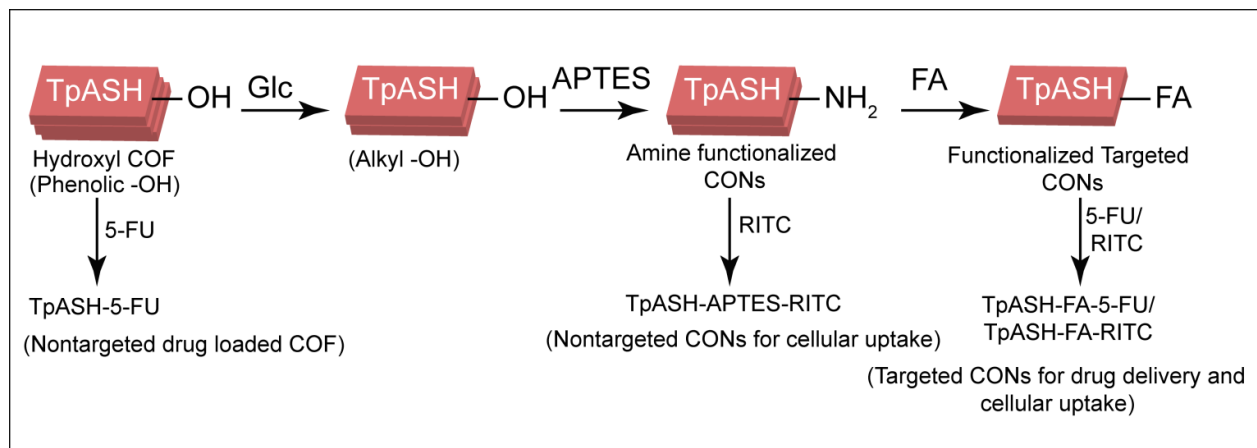


Figure S38. Schematic representation for targeted/non-targeted delivery component.

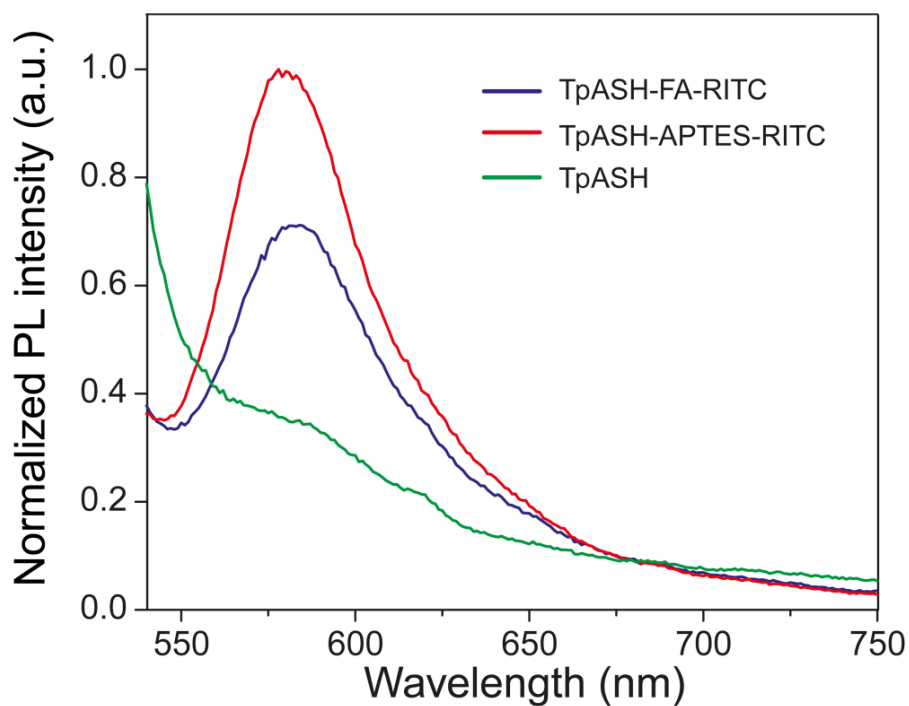


Figure S39. PL spectra of targeted fluorescent conjugated CONs (TpASH-FA-RITC) and non-targeted fluorescent conjugated CONs (TpASH-APTES-RITC). The samples grafted with RITC. Emission spectra is noted at 540 nm excitation wavelength.

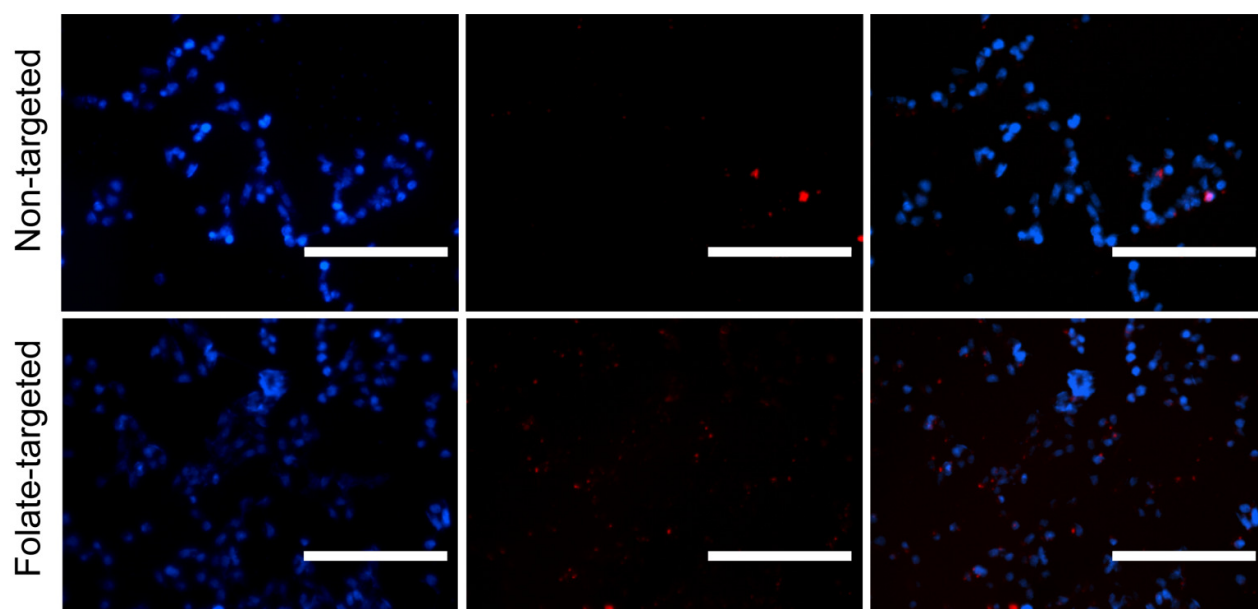


Figure S40. Cellular uptake studies of targeted CONs (TpASH-FA-RITC) and non-targeted CONs (TpASH-APTES-RITC) carried out on MDA-MB-231 cells. The cells were incubated with TpASH-FA-RITC and TpASH-APTES-RITC followed staining with DAPI. Interestingly the targeted CONs show preferential distribution compared to the non-targeted one as expected. (Scale bar: 50 μ m)

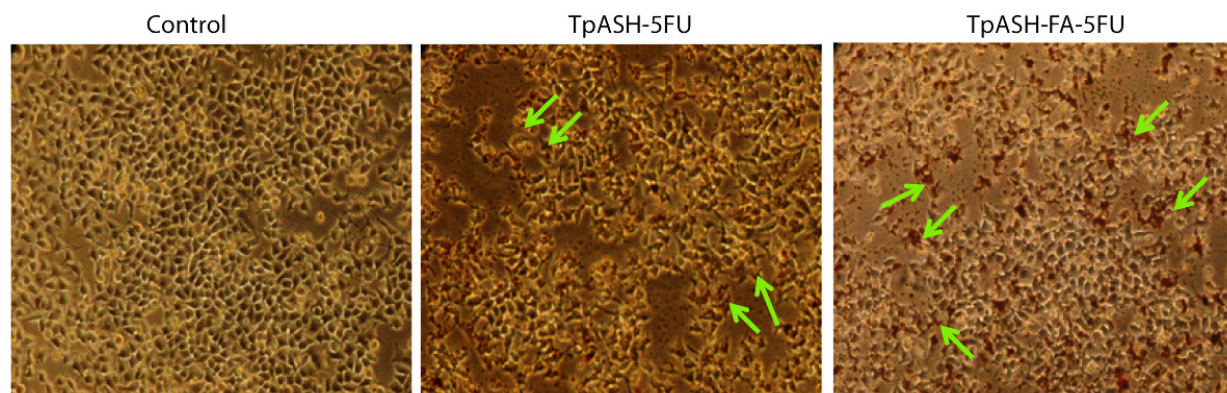


Figure S41. Comparison of apoptosis assay between control, TpASH-5FU and TpASH-FA-5FU; where TpASH-FA-5FU showed greater extent of apoptosis.

Section S-11: References

- [1] Yamada, H.; Kojo, M.; Nakahara, T.; Murakami, K.; Kakima, T.; Ichiba, H.; Yajima, T.; Fukushima, T. *Spectrochim. Acta Mol. Biomol. Spectrosc.* **2012**, *90*, 72-77.
- [2] Yelamaggad, C. V.; Achalkumar, A. S.; Shankar Rao, D. S.; Krishna Prasad, S.; *J. Org. Chem.* **2009**, *74*, 3168-3171.
- [3] Kandambeth, S.; Mallick, A.; Lukose, B.; Mane, V. M.; Heine, T.; Banerjee, R. *J. Am. Chem. Soc.* **2012**, *134*, 19524-19527.
- [4] a) Centore, R.; Carella, A.; Tuzi, A.; Capobianco, A.; Peluso, A. *CrystEngComm* **2010**, *12*, 1186-1193. b) Haider, A.; Akhter, Z.; Siddiqi, H. M.; Tiekink, E. R. T. *J. Chem. Cryst.* **2010**, *40*, 397-401.
- [5] Kargar, H.; Kia, R.; Tahir, M. N. *Acta Crystallogr Sect E Rep Online* **2012**, *68*, 2117.
- [6] Kandambeth, S.; Venkatesh, V.; Shinde, D. B.; Kumari, S.; Halder, A.; Verma, S.; Banerjee, R. *Nat. Commun.* **2015**, *6*, 6786.
- [7] a) Mitra, S.; Subia, B.; Patra, P.; Chandra, S.; Debnath, N.; Das, S.; Banerjee, R.; Kundu, S. C.; Pramanik, P.; Goswami, A. *J. Mater. Chem.* **2012**, *22*, 24145-24154. b) Guo, Y.; Wang, H.; He, C.; Qiu, L.; Cao, X. *Langmuir* **2009**, *25*, 4678-4684.
- [8] a) Del Campo, A.; Sen, T.; Lellouche, J. -P.; Bruce, I. J. *J. Magn. Magn. Mater.* **2005**, *293*, 33-40. b) Bruce, I. J.; Sen, T. *Langmuir* **2005**, *21*, 7029-7035.
- [9] Patra, P.; Mitra, S.; Das Gupta, A.; Pradhan, S.; Bhattacharya, S.; Ahir, M.; Mukherjee, S.; Sarkar, S.; Roy, S.; Chattopadhyay, S.; Adhikary, A.; Goswami, A.; Chattopadhyay, D. *Colloids Surf. B* **2015**, *133*, 88-98.